

SECURITY INFORMATION
CLASSIFICATION CANCELLED
~~RESTRICTED~~

UNCLASSIFIED RM L53A07

PT-30
NACA RM L53A07

Section Copy



RESEARCH MEMORANDUM

LIBRARY COPY

MAR 23 1990

LANGLEY RESEARCH CENTER
LIBRARY NASA, HAMPTON, VA.

COMPRESSIBLE-FLOW SOLUTIONS FOR THE ACTUATOR DISK

By James B. Delano and John L. Crigler

Langley Aeronautical Laboratory
Langley Field, Va.

CLASSIFICATION CANCELLED
BY AUTHORITY J. W. CROWLEY
CHANGE #1667 DATE 12-7-53 T.C.F.

CLASSIFIED DOCUMENT

This material contains information affecting the National Defense of the United States within the meaning of the espionage laws, Title 18, U.S.C., Secs. 793 and 794, the transmission or revelation of which in any manner to an unauthorized person is prohibited by law.

NATIONAL ADVISORY COMMITTEE FOR AERONAUTICS

WASHINGTON

March 20, 1953

~~RESTRICTED~~
UNCLASSIFIED

NATIONAL ADVISORY COMMITTEE FOR AERONAUTICS

RESEARCH MEMORANDUM

COMPRESSIBLE-FLOW SOLUTIONS FOR THE ACTUATOR DISK

By James B. Delano and John L. Crigler

SUMMARY

Generalized solutions for the actuator disk in subsonic compressible flow have been obtained and the compressible- and incompressible-flow phenomena are compared. The results show large differences in the flow variables across the disk.

Two primary types of solutions were obtained: one wherein the flow immediately behind the disk is subsonic and the other wherein this flow is supersonic. For the subsonic wake, the maximum efficiencies for compressible and incompressible flow are the same up to choked flow. The maximum efficiencies for the supersonic wake are lower than for the subsonic wake but this difference decreases as the free-stream Mach number approaches 1.0.

The use of actuator disks in tandem is one method of delaying the large losses in efficiency associated with choked flow, especially at low values of Mach number and high loadings. A level of efficiency almost as high as for incompressible flow could be maintained until the flow in all disks became choked. A single actuator disk gives the ideal efficiency only for power loadings up to those required to choke the flow.

INTRODUCTION

The simple momentum theory has been used to great advantage in analyzing propeller problems and predicting propeller efficiencies for known operating conditions. In the simple momentum theory the propeller has been treated as an actuator disk in incompressible flow with the thrust of the propeller uniformly distributed over the disk and with a constant axial interference velocity over the disk. Since, in practice, propellers must operate in compressible flow, it was felt that an extension of the actuator-disk theory to compressible flow might prove useful. Consequently, the simple momentum theory for an actuator disk has been extended to compressible flow based on what appear to be the logical assumptions.

~~RESTRICTED~~
UNCLASSIFIED

If a large pressure change is assumed to occur across the disk and this change occurs isentropically, then a large density change must also occur. Under these conditions, obviously, an increase in density across the disk must also be accompanied by a decrease in velocity through the disk to satisfy the conservation of mass flow. Solutions for the actuator disk in compressible flow are presented in reference 1 for one Mach number and for a limited range of power loading. The study of reference 1 did not include the possibility that the flow anywhere in the stream have a Mach number greater than 1.

A more comprehensive study of the flow phenomena and performance characteristics for an actuator disk in compressible flow is presented herein. The scope of the treatment has been extended to include the effect of entropy changes associated with profile and shock losses. In addition, a study is made of the conditions under which the flow in the slipstream exceeds a Mach number of 1.0, and the performance of the disk is calculated.

SYMBOLS

a	speed of sound, $\left(\frac{\gamma p}{\rho}\right)^{1/2}$, ft/sec
A	slipstream cross-sectional area
E	total energy, ft-lb/slug
g	acceleration of gravity
H	total pressure, lb/sq ft
m	mass flow, slug/sec
M	Mach number in slipstream
M_{2n}	Mach number behind normal shock
p	static pressure, lb/sq ft
Δp	static-pressure rise through disk, $p_2 - p_1$, lb/sq ft
P	total power added to slipstream by actuator disk, ft-lb/sec
P_i	power producing thrust, ft-lb/sec

P_o power expended in profile or shock losses in the disk,
ft-lb/sec

P_c power disk-loading coefficient, $\frac{P}{\frac{1}{2}\rho_o V_o^3 A_1}$

P_{c_i} power disk-loading coefficient, $\frac{P_i}{\frac{1}{2}\rho_o V_o^3 A_1}$

P_{c_o} power disk-loading coefficient, $\frac{P_o}{\frac{1}{2}\rho_o V_o^3 A_1}$

P_c^* value of P_c when the flow becomes choked

T thrust, lb

T_c thrust disk-loading coefficient, $\frac{T}{\frac{1}{2}\rho_o V_o^2 A_1}$

V velocity in slipstream, ft/sec

γ ratio of specific heats (for air, 1.4)

ρ air density, slugs/cu ft

η efficiency, $\frac{TV_o}{P} = \frac{T_c}{P_c}$

η_i ideal induced efficiency for compressible flow

$\eta_{i_{inc}}$ ideal induced efficiency for incompressible flow
 $\left(\text{from } P_{c_i} = \frac{4(1 - \eta_{i_{inc}})}{3} \right)$

Subscripts:

0 station far ahead of disk

1 station immediately ahead of disk

2 station immediately behind disk
3 station far behind disk
F conditions pertaining to front disk of disks in tandem
R conditions pertaining to rear-disk of disks in tandem
s solution for supersonic wake

THEORY

Basic Assumptions and Considerations

The actuator disk and the stations used in the analysis are shown in figure 1. The assumptions made in reference 1 are used herein. These assumptions are:

- (a) The propeller may be represented by an actuator disk of zero thickness.
- (b) The velocity distribution over any cross section of the stream-tube passing through the disk is taken to be uniform (one-dimensional flow).
- (c) The energy is added to the slipstream instantaneously and uniformly over the disk.
- (d) The slipstream area is continuous through the disk so that the cross-sectional areas immediately ahead of and immediately behind the disk are equal.
- (e) The actuator disk introduces no rotation in the slipstream.
- (f) In the final wake the static pressure returns to the free-stream value ($p_3 = p_0$).
- (g) The flow ahead of the disk is isentropic.

The scope of the treatment has been extended to include solutions wherein arbitrary energy losses, such as might be associated with blade profile drag, occur at the actuator disk. The solutions presented herein are for free-stream subsonic flows wherein the Mach number immediately ahead of the disk does not exceed 1.0. In order for M_1 to reach values greater than 1.0, the slipstream must contract and then expand ahead of

the disk (similar to the shape of a Laval nozzle) with a Mach number of 1.0 at the minimum cross section. This type of flow seemed highly unlikely for a free boundary even though pressure waves from the disk could possibly travel upstream outside the slipstream boundary.

The addition of power greater than that required to produce $M_1 = 1.0$ is assumed, therefore, to cause no further changes in the flow upstream of the disk. With this assumption, solutions of the problem consistent with the preceding assumptions are possible only for nonisentropic flow between stations 1 and 3. Under such conditions, depending upon the assumed distribution of the losses between stations 1 and 3 there are two possibilities: (a) the Mach number M_2 immediately behind the disk (station 2, see. fig. 1) may decrease or (b) it may become supersonic. The possibility of a supersonic wake has received some consideration in reference 2.

Solutions have been obtained under the assumption of both subsonic and supersonic exit velocities, and the power disk loading of the probable change from subsonic flow to supersonic flow behind the disk, for a given stream Mach number, has been determined.

Method of Solution and Basic Equations

Subsonic wake.— Figure 1 defines the four stations in the slipstream studied in the course of the analysis. Free-stream conditions, which are known, exist at station 0. Stations 1 and 2, respectively, are immediately ahead of and immediately behind the disk. The power is added to the slipstream between stations 1 and 2. Station 3 is in the final wake where the static pressure is again equal to the free-stream static pressure. The problem is to determine the flow variables throughout the slipstream associated with given free-stream conditions and power disk loading.

The solution for a given set of operating conditions is obtained when the flow variables satisfy the thrust, energy, and continuity relationships. Since the relationships of the various flow variables are not explicit, a method of successive approximations is employed to effect a solution. The following method of solution was employed.

A tentative assumption of Mach number at station 1 permits the determination of all the flow variables at station 1 from isentropic considerations. The variation of streamtube cross-sectional area with Mach number for isentropic flow is given in reference 3 as

$$\frac{A_1}{A_0} = \frac{M_0}{M_1} \left(\frac{1 + \frac{\gamma-1}{2} M_1^2}{1 + \frac{\gamma-1}{2} M_0^2} \right)^{\frac{\gamma+1}{2(\gamma-1)}} \quad (1)$$

The value of M_1 is never assumed to be greater than 1.0 for the final results presented in this paper for the reasons previously stated. The static pressure p_1 is obtained from the isentropic relations between the total and static pressures between station 0 and 1 given by

$$\frac{H_1}{p_1} = \left(1 + \frac{\gamma-1}{2} M_1^2 \right)^{\frac{\gamma}{\gamma-1}} \quad (2)$$

and

$$H_0 = H_1 \quad (3)$$

The density at station 1 is obtained from the isentropic pressure-density relation

$$\frac{\rho_1}{\rho_0} = \left(\frac{p_1}{p_0} \right)^{1/\gamma} \quad (4)$$

The velocity V_1 is obtained from the continuity of mass flow

$$\frac{V_1}{V_0} = \frac{\rho_0}{\rho_1} \frac{A_0}{A_1} \quad (5)$$

The total energy at station 0 is equal to the total energy at station 1 and is given by

$$\left. \begin{aligned} E_0 &= E_1 \\ E_0 &= \frac{V_0^2}{2} + \frac{\gamma}{\gamma-1} \frac{p_0}{\rho_0} \\ E_1 &= \frac{V_1^2}{2} + \frac{\gamma}{\gamma-1} \frac{p_1}{\rho_1} \end{aligned} \right\} \quad (6)$$

The flow variables at station 3 are found next. These variables depend on the amount of energy being added to the slipstream at the disk, how this energy is added (isentropic or nonisentropic compression), and the mass flow. The total energy at station 3 is equal to that at station 1 plus the energy added by the disk.

Since $\frac{P}{\rho_1 A_1 V_1}$ is the power per unit mass flow added to the stream by the disk,

$$\frac{V_0^2}{2} + \frac{\gamma}{\gamma - 1} \frac{P_0}{\rho_0} + \frac{P}{\rho_1 A_1 V_1} = \frac{V_3^2}{2} + \frac{\gamma}{\gamma - 1} \frac{P_3}{\rho_3} \quad (7)$$

This equation can be rearranged to give

$$\frac{P}{\rho_1 A_1 V_1} = \frac{V_3^2 - V_0^2}{2} + \frac{\gamma}{\gamma - 1} \frac{P_0}{\rho_0} \left(\frac{\rho_0}{\rho_3} - 1 \right)$$

The total power can be divided into two parts

$$P = P_1 + P_0 \quad (8)$$

where

$$\frac{P_1}{\rho_1 A_1 V_1} = \frac{V_3^2 - V_0^2}{2} \quad (9)$$

is the power per unit mass flow required to produce thrust and

$$\frac{P_0}{\rho_1 A_1 V_1} = \frac{\gamma}{\gamma - 1} \frac{P_0}{\rho_0} \left(\frac{\rho_0}{\rho_3} - 1 \right) \quad (10)$$

is the additional power associated with entropy changes resulting from profile or shock losses in the disk.

For the case where no entropy change takes place, $\rho_3 = \rho_0$ and hence $P_0 = 0$. Then, only induced losses are incurred and $P = P_1$. The velocity at station 3 can be obtained from equation (9). When P_1 is changed to the power disk-loading coefficient P_{c1} , the velocity ratio becomes

$$\frac{V_3}{V_0} = \left(1 + \frac{P_{c1}}{A_0/A_1} \right)^{1/2} \quad (11)$$

Similarly, the density ratio $\frac{\rho_0}{\rho_3}$ can be obtained from equation (10) which can be put in the following form:

$$\frac{\rho_0}{\rho_3} = 1 + \frac{(\gamma - 1)}{2} M_0^2 \frac{P_{c0}}{A_0/A_1} \quad (12)$$

also

$$P_c = P_{c1} + P_{c0} \quad (13)$$

The speed of sound at station 3 is given by

$$a_3 = \sqrt{\frac{\gamma P_3}{\rho_3}} \quad (14)$$

and the Mach number is given by

$$M_3 = \frac{V_3}{a_3} \quad (15)$$

The total pressure is found from

$$\frac{H_3}{P_3} = \left(1 + \frac{\gamma - 1}{2} M_3^2 \right)^{\frac{\gamma}{\gamma - 1}} \quad (16)$$

where $P_3 = P_0$. The area ratio is given by

$$\frac{A_3}{A_0} = \frac{\rho_0 V_0}{\rho_3 V_3} \quad (17)$$

All the flow variables at station 3 have now been determined for the assumed M_1 and for the given power per unit mass flow, that is, P_c is constant.

Conditions at station 2 are next determined by isentropic-flow relations in working backwards from station 3 to station 2. The area ratio A_3/A_2 is given by

$$\frac{A_3}{A_2} = \frac{A_3}{A_1} = \frac{\rho_1 V_1}{\rho_3 V_3} \quad (18)$$

When isentropic flow occurs across the disk, ρ_3 equals ρ_0 . The Mach number at station 2 is determined from the area ratio

$$\frac{A_3}{A_2} = \frac{M_2}{M_3} \left(\frac{1 + \frac{\gamma-1}{2} M_3^2}{1 + \frac{\gamma-1}{2} M_2^2} \right)^{\frac{\gamma+1}{2(\gamma-1)}} \quad (19)$$

The static pressure p_2 is obtained from

$$\frac{H_2}{p_2} = \left(1 + \frac{\gamma-1}{2} M_2^2 \right)^{\frac{\gamma}{\gamma-1}} \quad (20)$$

where

$$H_2 = H_3 \quad (21)$$

The density at station 2 is obtained from

$$\frac{\rho_2}{\rho_3} = \left(\frac{p_2}{p_0} \right)^{1/\gamma} \quad (22)$$

The velocity V_2 is obtained from the continuity of mass flow

$$V_2 = \frac{\rho_1 V_1}{\rho_2} \quad (23)$$

since $A_1 = A_2$. The energy at station 2 is equal to the energy at station 3 and is given by

$$\left. \begin{aligned} E_2 &= E_3 \\ E_2 &= \frac{V_2^2}{2} + \frac{\gamma}{\gamma - 1} \frac{P_2}{\rho_2} \\ E_3 &= \frac{V_3^2}{2} + \frac{\gamma}{\gamma - 1} \frac{P_3}{\rho_3} \end{aligned} \right\} \quad (24)$$

The determination of the flow variables at station 2 is now complete for the assumed value of M_1 .

The corresponding value of thrust consistent with the assumed value of M_1 , P_c , and P_{c_0} is found from the sum of the pressure forces and momentum changes across the disk

$$T = \rho_1 A_1 V_1 (V_2 - V_1) + (P_2 - P_1) A_1 \quad (25)$$

It can be shown, however, by methods similar to those shown in reference 4 that the net pressure force on the fluid between stations 0 and 3 must be zero. For this condition, the thrust is given also by the change in momentum between stations 0 and 3

$$T = \rho_1 A_1 V_1 (V_3 - V_0) \quad (26)$$

In general, the arbitrarily assumed value of M_1 associated with a given value of P_c and P_{c_0} will not satisfy equation (26). The correct final solution will be obtained when M_1 has been chosen in such a way that equations (25) and (26) give the same value of thrust. If the thrusts given by these two independent thrust equations (25) and (26) are plotted against M_1 for given values of P_c and P_{c_0} , the intersections of the two curves will give the solution.

The thrust loading T/A_1 obtained from the two independent thrust equations (25) and (26) is shown plotted in figure 2 against M_1 for constant values of P_c , P_{c_0}/P , and free-stream Mach number. Three typical cases are presented to show the types of solutions obtained. In figure 2(a) there are two values of M_1 (one subsonic and one supersonic) that satisfy the two independent thrust equations; hence, there

are two possible solutions. In line with the previous discussion, only the subsonic values of M_1 will be used. In figure 2(b) there are no crossings of the two thrust curves and thus no solutions. This fact indicates that there is a limit to the maximum power disk loading for which solutions can be obtained for isentropic flow throughout the slipstream. For example, if a sufficient part of the power had gone into losses, a solution would have been possible, such as is shown in figure 2(c). In figure 2(c) all conditions are the same as in figure 2(b) except that the power loss P_o/P (drag or shock loss) is 26.4 percent of the total power. In this case only one solution was obtained and that is for $M_1 = 1.0$. If P_o/P is increased for the same values of P_c and M_o , two solutions will be obtained, one with M_1 subsonic and one with M_1 supersonic.

These results can be summarized as follows: When P_c is less than P_c^* , there are two values of M_1 (one subsonic and one supersonic) that will satisfy the two independent thrust equations. When P_c is equal to P_c^* , there is only one value of M_1 that produces a solution, that is, $M_1 = 1.0$, and the flow is everywhere isentropic. When P_c is greater than P_c^* , no solutions are possible unless arbitrary losses are introduced in the disk. These losses are similar to losses associated with the blade profile drag and shocks. Consequently, the flow through the disk is no longer isentropic.

Thus far only solutions having subsonic wakes have been considered. It will be shown later under "Results and Discussion" that there is a transition from a subsonic wake to a supersonic wake at some value of P_c greater than P_c^* , that is, after the flow into the disk becomes choked.

Supersonic wake.— In order to analyze the flow behind the disk with a supersonic wake, the flow out of the disk is assumed to be similar to the supersonic flow out of a nozzle in which the discharge or exit pressure is less than the ambient pressure at the exit. The attendant shock formations in the wake are discussed in detail in reference 3 (pp. 172-174). This compression gives rise to shock losses in the wake so that the treatment used for the subsonic-wake solutions no longer is applicable. The following method has been used to obtain the supersonic-wake solutions.

All the flow factors through station 1 have been determined since the flow is choked. A value of $V_2 (M_2 > 1.0)$ is assumed. The density at station 2 is obtained from the continuity of mass flow

$$\rho_2 = \frac{\rho_1 V_1}{V_2}$$

In general, by assuming $\frac{P}{m}$, p_2 can be obtained from the energy equation

$$E_0 + \frac{P}{m} = E_2$$

or

$$\frac{V_0^2}{2} + \frac{\gamma}{\gamma - 1} \frac{p_0}{\rho_0} + \frac{P}{m} = \frac{V_2^2}{2} + \frac{\gamma}{\gamma - 1} \frac{p_2}{\rho_2} \quad (27)$$

The speed of sound is given by

$$a_2 = \sqrt{\frac{\gamma p_2}{\rho_2}}$$

and the Mach number by

$$M_2 = \frac{V_2}{a_2}$$

The thrust is given by the sum of the pressure forces and momentum changes across the disk

$$\frac{T}{m} = V_2 - V_1 + \frac{p_2 - p_1}{\rho_1 V_1}$$

which is another form of equation (25). The efficiency is given by

$$\eta = \frac{\frac{T}{m} V_0}{\frac{P}{m}}$$

The power disk-loading coefficient is given by

$$P_c = \frac{\frac{P}{m} \frac{A_0}{A_1}}{\frac{V_0^2}{2}}$$

The solution for obtaining all the flow variables across the disk, the efficiency, and power disk-loading coefficient is now complete. It is not necessary to make a detailed analysis of a balance of energy and thrust by comparing the total energy and thrust at stations 2 and 3.

The arbitrary assumption of V_2 and $\frac{P}{m}$ produces an infinite number of solutions which in general do not represent the maximum-efficiency case. The maximum efficiency, however, is of particular interest and occurs when the flow through the disk is isentropic. For this case, p_2 is obtained from the isentropic pressure-density relation

$$p_2 = p_1 \left(\frac{\rho_2}{\rho_1} \right)^\gamma$$

The value of $\frac{P}{m}$ corresponding to this isentropic process can now be obtained directly from equation (27). It is to be noted that in the subsonic-wake case, there is a definite limit to the value of the power ($P_c = P_c^*$) the disk can absorb isentropically. For the supersonic-wake case, however, much larger amounts of power can be absorbed isentropically by the disk.

RESULTS AND DISCUSSION

Ideal Solutions

Solutions of the flow variables throughout the slipstream are presented in figures 3 to 8 for forward Mach numbers of 0.60, 0.70, 0.80, 0.85, 0.90, and 0.95. These results are presented as Mach number and as ratios of pressure, density, velocity (referred to free-stream conditions), and ratio of cross-sectional area of the slipstream (referred to the area of the actuator disk), all as functions of the power disk-loading coefficient P_c . The variation of efficiency with P_c is presented in the same figures as the pressure ratios. When the flow into

the disk is subsonic ($M_1 < 1$), the flow behind the disk (station 2) must be subsonic, as will be shown later, and only the solutions for a subsonic wake were obtained. When the flow into the disk becomes choked ($M_1 = 1$), solutions were obtained for both subsonic and supersonic flows at station 2. For the subsonic-wake case, however, solutions can be obtained only by introducing losses in the disk. All curves for solutions with subsonic flow at station 2 are marked with plain symbols while the curves obtained for supersonic flow at station 2 are marked with symbols having subscript s (figs. 5 to 8). Choked flow occurs at the lower value of P_c at which there is a sharp break in the curves.

There is a range of power disk-loading coefficient for which both subsonic and supersonic wakes appear as alternative possibilities. Since there is nothing in the equations to indicate which type of flow might occur and which efficiency might be obtainable, the results were studied to determine when the change from a subsonic wake to a supersonic wake could be expected. A supersonic wake is possible for all exit velocities for which a shock pattern exists at the exit or extends downstream from the exit. The lowest supersonic-wake Mach number which can exist is seen by analogy with nozzle flow to correspond to the condition of a normal shock immediately behind the actuator disk or at the exit of a supersonic nozzle. In this case, except for an infinitesimal distance behind the actuator disk, the wake flow is actually subsonic. Consequently, the subsonic-wake calculations should be applicable to this case and the losses which it is necessary to assume in order to obtain a solution correspond to the losses in a normal shock at the exit.

A direct calculation of the Mach number immediately behind the disk for the case with a normal shock at the exit is difficult to make because the boundary pressure at the exit is not known at this stage of the calculation. However, since the subsonic- and supersonic-wake calculations should give the same results (corresponding efficiencies and powers are equal) for the normal shock at the exit, the intersection of the efficiency curves for the two types of solution (subsonic- and supersonic-wake solutions) should correspond to the condition of a normal shock at the exit. In figure 9, the Mach number behind a normal shock is plotted against the Mach number in front of a normal shock (see data from table 3 of ref. 3); this relation is shown by the solid line. The abscissas of the individual points (shown by symbols) which are plotted in figure 9 are the values of M_2 from the subsonic-wake solutions at the point of intersection of the efficiency curves for the subsonic-wake and supersonic-wake solutions. The ordinates of these points are the values of $(M_2)_s$ taken from the supersonic-wake solutions at the corresponding conditions. It is seen that the relation between

the subsonic and supersonic values of M_2 at the point of intersection of the efficiency curves is exactly that for a normal shock.

The curves, figures 5 to 8, for all flow parameters are shown as solid lines for the subsonic-wake solutions up to the transition value of P_c and as dashed lines at higher values of P_c . The solutions for the supersonic wake are shown as solid lines, beginning at the value of P_c for equal efficiencies from the two wake solutions and all higher values of P_c . At lower values of P_c , the solutions for the supersonic wake are shown as dashed lines and are presented only to show the range of calculations.

The curves in figures 3 to 8 for compressible flow show two important discontinuities of the flow parameters. The first discontinuities occur at the value of P_c at which $M_1 = 1.0$ which is called the critical power disk-loading coefficient and is designated as P_c^* . Choking cannot occur for the incompressible-flow case; therefore, the mass flow can increase indefinitely as P_c is increased, whereas for compressible flow the mass flow reaches a maximum for a given forward Mach number when the Mach number immediately ahead of the disk reaches a value of 1.0. The second break in the curves occurs at the value of P_c where the efficiency for the subsonic-wake solution is equal to the efficiency for the supersonic-wake solution.

Curves for the supersonic-wake solutions are not included for the lower Mach numbers (figs. 3 and 4). In these cases extremely high power disk loadings are required to choke the flow and supersonic calculations for choked flow were not presented as it was felt the power disk loadings were beyond the practical range for propeller operation.

Pressure. - The pressure rise through the disk for compressible and incompressible flow at power disk loadings below choking is compared at several forward Mach numbers in figure 10 for maximum-efficiency conditions (no profile losses). For a given value of P_c and M_0 , the pressure rise through the disk is much greater for compressible flow than for incompressible flow. The figure shows that the pressure rise for compressible flow is $\frac{1}{(1 - M_0^2)}$ times that for incompressible flow at

light power loadings. The (a) parts of figures 5 to 8 also show that, for a given forward Mach number when the flow into the disk reaches a Mach number of 1.0, practically no additional pressure rise can be obtained even for large increases in power for the subsonic-wake solutions. The same figures also show a large decrease in pressure across the disk for the supersonic-wake solutions.

Density.- The changes in density are similar to the changes in pressure.

Velocity and Mach number.- The velocity changes are similar to the Mach number changes throughout the slipstream. The velocity in front of the disk is much greater than the incompressible-flow value and the difference increases with P_c up to choking. (See fig. 6(c).) The most significant result is the great drop in velocity through the disk for the subsonic-wake solution, and the great increase in velocity for the supersonic-wake solution. The effect of forward Mach number and power disk loading on the velocity immediately behind the disk is presented in figure 11 for the subsonic-wake case. This figure shows that the velocity immediately behind the disk is less than the free-stream velocity for high subsonic Mach numbers for all power disk loadings. At lower free-stream Mach numbers (e.g., $M_0 \approx 0.65$ to 0.69) the velocity behind the disk is greater than the free-stream velocity.

Figure 12 shows a comparison of the average-velocity ratio through the disk for incompressible and compressible flows up to choking. The average velocity through the disk $\frac{V_1 + V_2}{2}$ is higher for compressible flow than for incompressible flow, and increases with P_c . At low power loadings, however, there is not much difference.

From the great differences in the flow factors for incompressible and compressible flow the use of conventional incompressible-flow theory for propellers might be expected to give erroneous results in calculating propeller performance characteristics. Comparison of experimental and calculated results, however, for propellers even at high subsonic Mach numbers has shown remarkably good agreement in over-all characteristics for light loadings. This good agreement may be due to the fact that the average of V_1 and V_2 for compressible and incompressible flow is not greatly different for light power loadings. For high power loadings, however, experimental propeller characteristics may differ greatly from calculations based on incompressible-flow theory.

Efficiency.- Figure 13 shows the variation of efficiency with power disk-loading coefficient for all free-stream Mach numbers for both the subsonic- and supersonic-wake solutions. The changes in efficiency for a given free-stream Mach number were discussed earlier in connection with transition of the flow from a subsonic to a supersonic wake. The drop in efficiency from the subsonic- to supersonic-wake case (transition drop) becomes less as the free-stream Mach number increases. Consequently, at the high subsonic Mach numbers the efficiency level is quite high for the supersonic wake case.

In figure 13 one maximum efficiency point obtained in experiments in the Langley 16-foot transonic tunnel is included for a free-stream Mach number of 0.96 and $P_c = 0.054$ for comparison with actuator-disk results. This efficiency falls between the lines representing the subsonic-wake solution with the flow choked and the supersonic-wake solution. This efficiency is about 16 percent lower than the ideal efficiency calculated for the supersonic wake and this loss represents approximately the blade profile-drag loss. The rest of the losses would appear even without blade profile-drag losses and would show up as shock losses in the wake. The efficiency and power disk-loading coefficient obtained for this propeller show that this propeller has a supersonic wake immediately behind the propeller plane.

Effect of Additional Losses

Subsonic wake.— Important effects are produced when additional losses are included in the analysis. These effects are shown in figure 14 for a forward Mach number of 0.85 and for values of P_o/P of 0, 0.1, 0.2, and 0.3 for the subsonic-wake case. For a given value of P_c the deviation of the flow factors from the free-stream values decreases as the profile losses are increased. For a fixed value of P_o/P , the limit of the subsonic-wake solution occurs when the Mach number M_1 into the disk reaches a value of 1.0. This limiting condition represents choked flow. The locus of similar limiting points for all values of P_o/P is designated as the "choke line." The choke lines are shown as dashed lines in figure 14. Once the flow becomes choked and the power is increased, solutions can only be obtained by the addition of further arbitrary losses in the disk, that is, choking occurs at higher values of P_c . Transition of the flow from a subsonic to a supersonic wake must occur somewhere along the choke lines.

The effect of additional losses on efficiency is shown in figure 15 for forward Mach numbers from 0.70 to 0.95 for the subsonic wake. The variation of efficiency for constant values of P_o/P is shown by the dashed lines. It can be shown that the efficiency is given by

$$\frac{\eta}{\eta_{P_o=0}} = 1 - \frac{P_o}{P} \quad \text{where} \quad \eta_{P_o=0} \quad \text{is the value of } \eta \quad \text{when} \quad \frac{P_o}{P} = 0 \quad \text{for the}$$

value of P_c under consideration. As P_c is increased above the value required to choke the flow, the efficiency decreases rapidly.

Supersonic wake.— Similarly, for the supersonic-wake case, the addition of profile-losses results in lower efficiencies than shown in

figure 13. The value of P_c at which choking occurs will increase with an increase of profile loss and the transition of flow from a subsonic to a supersonic wake will occur at some point along the choke line at a higher value of P_c than the transition for the zero-profile-loss case.

Previously, it was pointed out that the loss in efficiency associated with transition of flow from a subsonic wake to a supersonic wake decreases as the free-stream Mach number is increased. Consequently, it is evident that if sufficient power is added to produce a supersonic wake, even at a free-stream Mach number of 0.8, a very large loss in efficiency results (from 96 percent down to 70 percent, see fig. 13). The problem of particular importance, then is the determination, if possible, of methods to increase the efficiency by delaying the adverse effects associated with choking the flow. This can be done by the use of actuator disks in tandem.

Actuator Disks in Tandem

Solutions for actuator disks in tandem require knowledge of the flow field between the disks. In order to simplify this problem, it can be assumed that the disks are widely spaced and that only the mass flow passing through the first disk passes through the following disks. In addition, it is assumed that the final wake conditions of the leading disk are taken as the free-stream conditions of the following disk. Such a configuration resolves the problem into the solution of a series of single disks for which the solutions already obtained for a single disk can be used.

When a single actuator disk is operating at a condition where it is absorbing just enough power to produce choking, the addition of more power will produce a rapid decrease in efficiency. If, however, this additional power were absorbed by a second coaxial disk located far behind the first disk, it can be seen that the second disk could operate at a high level of efficiency as long as the flow into it were not choked. Consequently, the over-all efficiency of the two disks would be higher than for a single disk absorbing the same total power.

Solutions have been obtained for two, three, and an infinite number of disks in tandem using the methods presented in the appendix. No attempt was made to present all the flow factors since only the efficiency that can be obtained at high values of total power is of interest in the following analysis.

Calculations were made on the assumption that the flow through the leading disk has just choked. Additional power is then added only to the following disk until it becomes choked. The calculations were terminated for a finite number of disks when the flow into the last

disk became choked and, for an infinite number of disks, when the flow of the final wake reached a Mach number of 1.0. In this process the addition of power to any disk does not alter the flow conditions at any preceding disk. Each added disk becomes smaller than the preceding disk. This method of analysis was used for mathematical expediency and does not affect the results. For the case being considered ($M_0 = 0.80$), the diameter of the second disk was reduced about 3 percent and that of the third disk about 4 percent. The results of this analysis are presented in figure 16 for a forward Mach number of 0.80, as over-all efficiency against power disk-loading coefficient based on total-power, free-stream conditions for the front disk and the area of the front disk. The efficiency for tandem disks remains almost as high as the incompressible efficiency and is considerably higher than it is for the single disk absorbing the same total power. The efficiency for the tandem disks is lower than the incompressible value of efficiency because the mass flow into the tandem disks remains fixed as the power is allowed to increase. Choked flow for a single disk occurs at a value of $P_c = 0.174$ and the further addition of power results in a rapid loss in efficiency until the flow changes from a subsonic to a supersonic wake. For tandem disks this rapid loss in efficiency is delayed until the flow in all the disks is choked. Choked flow occurs at $P_c = 0.263$ for two disks, $P_c = 0.319$ for three disks, and $P_c = 0.584$ for an infinite number of disks. Thus, a considerable increase in high-efficiency power range results from the addition of one disk; further increases in power range occur for additional disks but this gain decreases as the number of disks is increased.

Since it was possible to obtain a high level of efficiency by adding the power in more than one disk, it is obvious that the efficiency obtained for a single actuator disk no longer represents the optimum or ideal efficiency for all operating conditions.

The use of closely spaced disks rather than widely spaced disks in tandem represents a practical propeller configuration. Experimental results show that final wake conditions are reached a short distance behind propellers and it is believed the results obtained with widely spaced disks are indicative of what may be expected for closely spaced propellers. Tests are needed to determine the effect of spacing on the performance of tandem propellers.

CONCLUDING REMARKS

Comparison of the incompressible- and compressible-flow phenomena show large differences in the flow variables across the actuator disk. For the case where only isentropic flow is considered for an actuator disk, the maximum efficiencies for compressible and incompressible flow

were found to be the same for power disk loadings up to those first required to choke the flow.

When the flow becomes choked, the further addition of power produces a rapid loss in efficiency. This loss in efficiency is associated with the transition of flow immediately behind the disk from subsonic to supersonic flow. When the flow immediately behind the disk is supersonic, the rate of efficiency loss with power disk loading is similar to but greater than that for incompressible flow.

The use of actuator disks in tandem is one method of delaying the large losses in efficiency associated with choked flow, especially at low values of Mach number and high loadings. A level of efficiency almost as high as for incompressible flow could be maintained until the flow in all disks became choked. It is obvious, therefore, that a single actuator disk gives the ideal efficiency only for power loadings up to those required to choke the flow.

Langley Aeronautical Laboratory,
National Advisory Committee for Aeronautics,
Langley Field, Va.

APPENDIX

SOLUTION OF SPECIAL CASE OF ACTUATOR DISKS IN TANDEM

For coaxial actuator disks in tandem any two successive disks are assumed to be far enough apart so that the final wake conditions of the front disk may be assumed to be the free-stream conditions of the following disk. The problem is simplified by the assumption that there are no profile or shock losses incurred. In addition, only the mass flow passing through the first disk is assumed to pass through all the disks. This assumption requires that the area of the second disk be smaller than the area of the first disk and just the right size to work on all the mass flow. These assumptions make possible the use of solutions already presented for the single actuator disk. Considerations similar to those of reference 4 show that the form of the general momentum equations involving thrust and boundary forces for this case remains the same and that the net boundary force is zero when the static pressures far in front of and far behind the actuator disks are the same. Figure 17 is a sketch of the stations used in this analysis.

The over-all thrust of the system is given by

$$T = m(V_{3R} - V_{0F}) \quad (1)$$

where V_{3R} is the final wake velocity of the rear disk and V_{0F} is the free-stream velocity of the front disk. The power ΔP added to the stream by any single disk is given by the change in energy from its free-stream to its final-stream conditions. Considering only an isentropic flow process this power is given by

$$\left(\frac{\Delta P}{m}\right)_n = \frac{1}{2}(V_3^2 - V_0^2)_n \quad (2)$$

where the subscript n refers to the n th disk. The total power P for all disks is given by

$$\frac{P}{m} = \sum_1^t \left(\frac{\Delta P}{m}\right)_n \quad (3)$$

where t equals total number of disks. It can be shown that

$$\frac{P}{m} = \frac{1}{2}(V_{3R}^2 - V_{0F}^2) \quad (4)$$

The total power disk-loading coefficient based on the free-stream conditions of the front disk and the area of the front disk is given by

$$P_c = \frac{\left(\frac{P}{m}\right)_m}{\frac{1}{2} \rho_{O_F} V_{O_F}^3 A_{1_F}}$$

which reduces to

$$P_c = \left(\frac{A_0}{A_1}\right)_F \left(\frac{V_{3R}^2}{V_{O_F}^2} - 1 \right) \quad (5)$$

The over-all efficiency is given by

$$\eta = \frac{m(V_{3R} - V_{O_F})V_{O_F}}{P}$$

which reduces to

$$\eta = \frac{2}{1 + \frac{V_{3R}}{V_{O_F}}} \quad (6)$$

For isentropic flow the final static pressure and density are the same as the initial free-stream values; consequently, equation (5) reduces to

$$P_c = \left(\frac{A_0}{A_1}\right)_F \left(\frac{M_{3R}^2}{M_{O_F}^2} - 1 \right) \quad (7)$$

and equation (6) reduces to

$$\eta = \frac{2}{1 + \frac{M_{3R}}{M_{O_F}}} \quad (8)$$

Equations (7) and (8) permit the calculation of the maximum performance for disks in tandem with isentropic flow throughout the stream. For these conditions the maximum value of M_{3R} can be 1.0 for an infinite

number of disks and the maximum value of $\left(\frac{A_0}{A_1}\right)_F$ is the value when the flow into the front disk is choked. Under these conditions the maximum values of P_c and η then become

$$P_{c_{\max}} = \left(\frac{A_0}{A_1}\right)_{F_{\max}} \left(\frac{1}{M_{OF}^2} - 1 \right) \quad (9)$$

and

$$\eta_{\max} = \frac{2}{1 + \frac{1}{M_{OF}}} \quad (10)$$

REFERENCES

1. Vogeley, Arthur W.: Axial-Momentum Theory for Propellers in Compressible Flow. NACA TN 2164 (corrected copy), 1951.
2. Klawans, Bernard B., and Vogeley, Arthur W.: A Cascade-General-Momentum Theory of Operation of a Supersonic Propeller Annulus. NACA RM L52J06, 1952.
3. Ferri, Antonio: Elements of Aerodynamics of Supersonic Flows. The MacMillan Co., 1949.
4. Glauert, H.: Airplane Propellers. The Axial Momentum Theory. Vol. IV of Aerodynamic Theory, div. I, ch. II, sec. 2, W. F. Durand, ed., Julius Springer (Berlin), 1935, pp. 184-187.

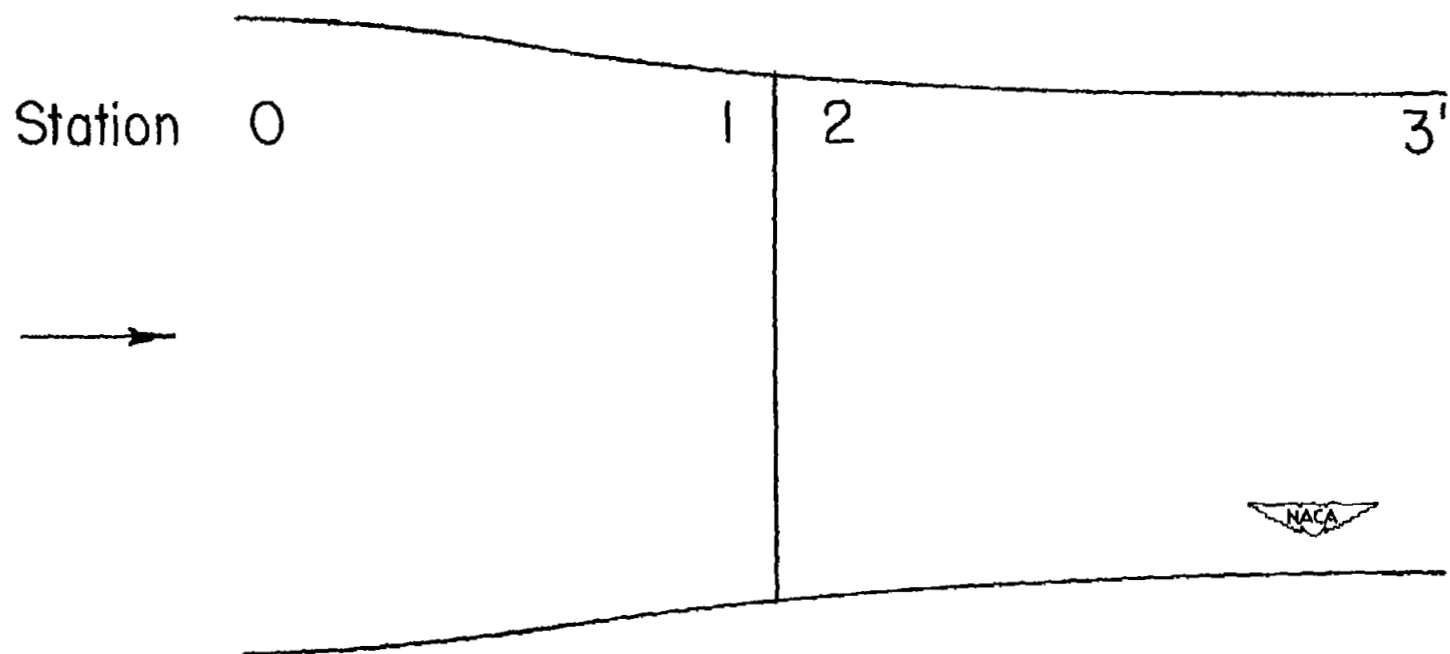


Figure 1.- Slipstream stations used in the analysis of single actuator disk. Free-stream conditions M , V , p , ρ , H , and E are given at station 0.

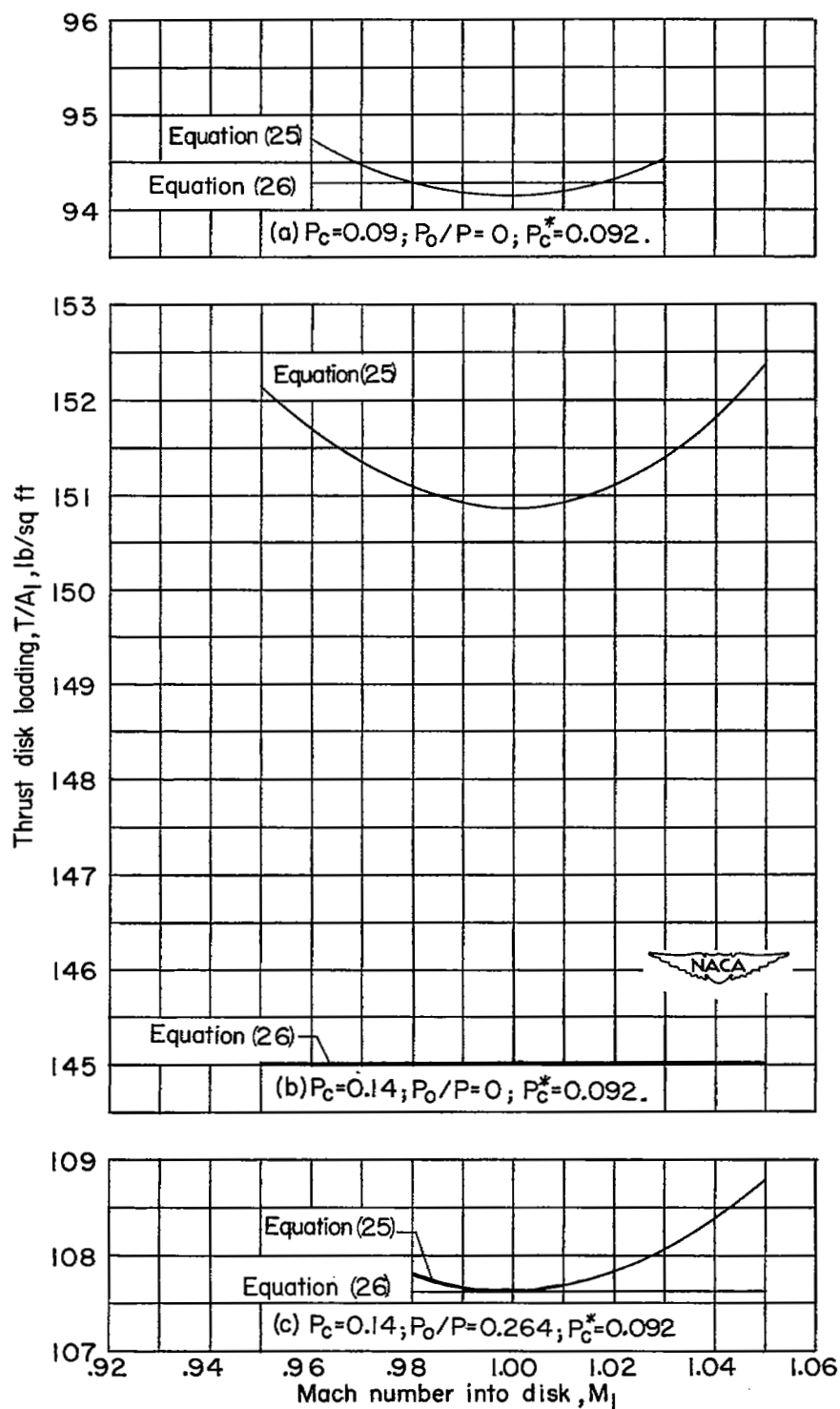
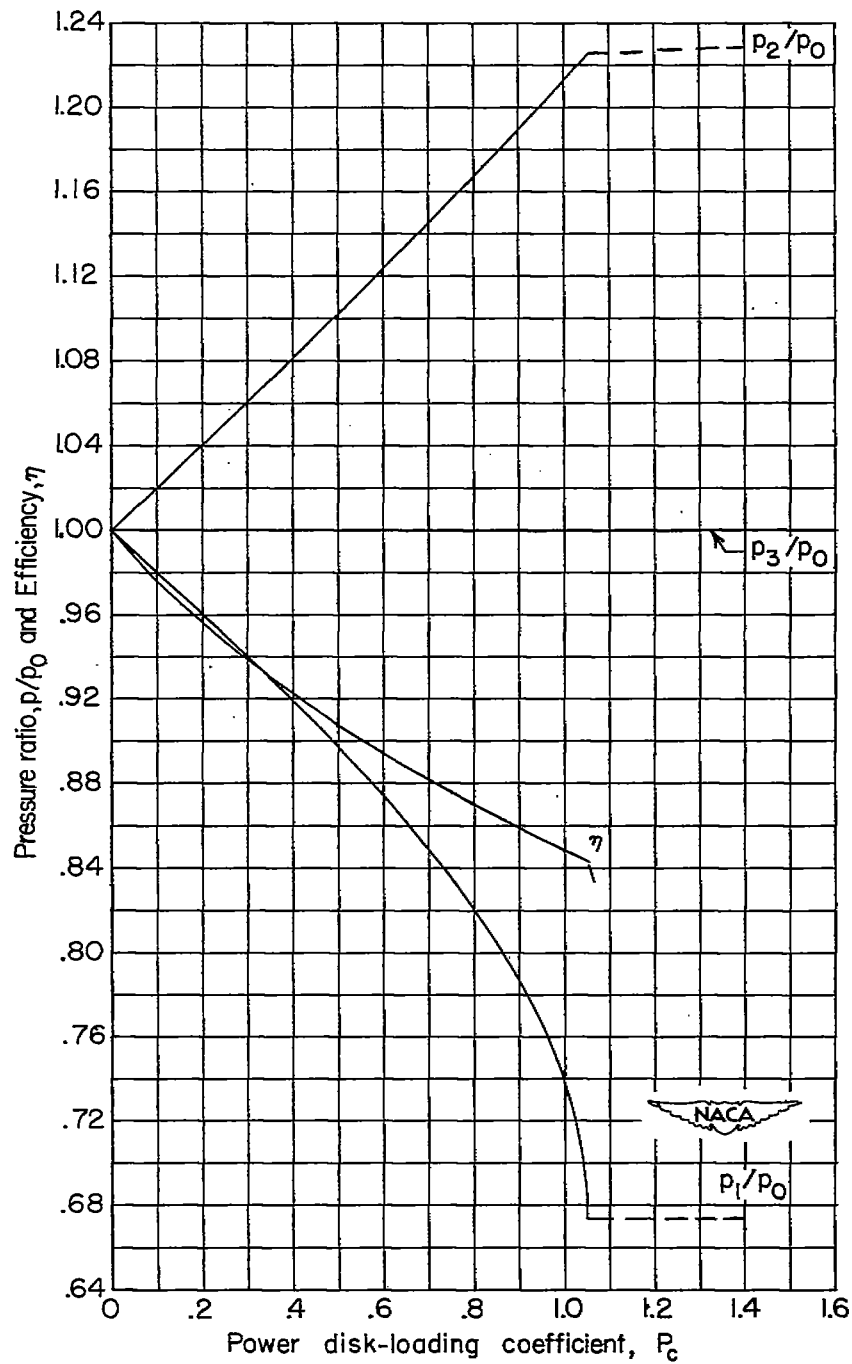
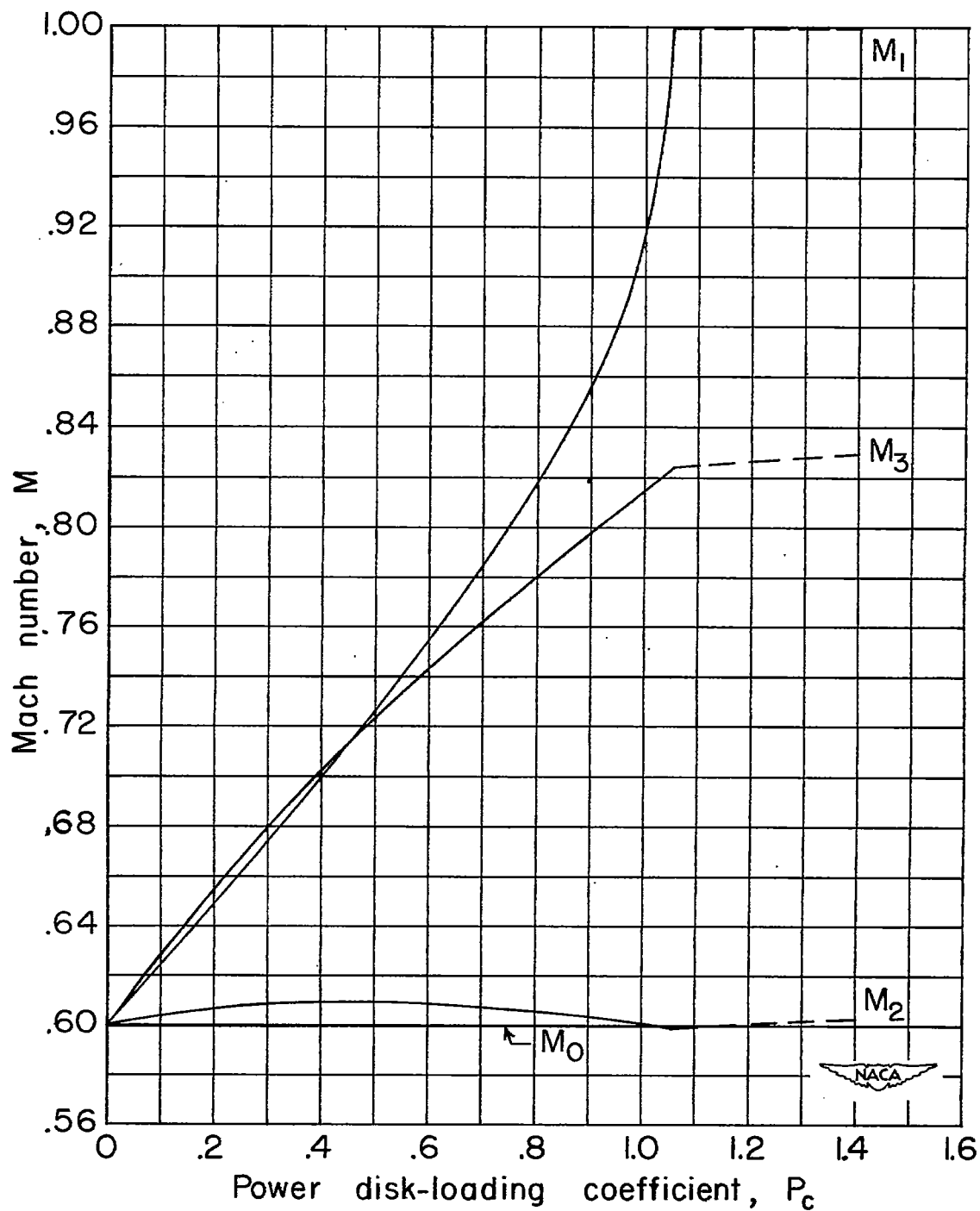


Figure 2.- Graphical solution to obtain thrust balance. $M_0 = 0.85$.



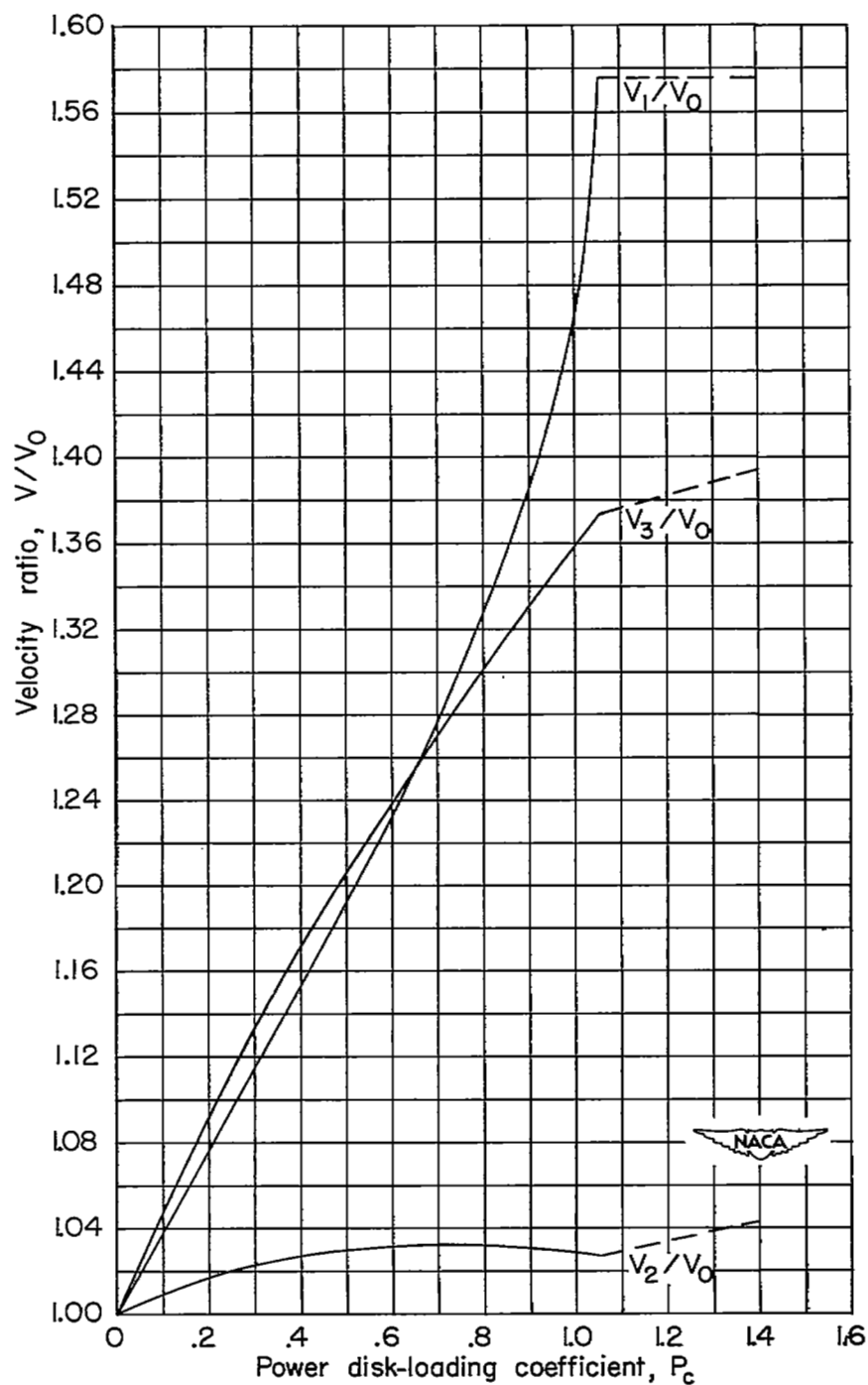
(a) Pressure ratio.

Figure 3.- Variation of slipstream flow factors with power loading.
 $M_0 = 0.60$.



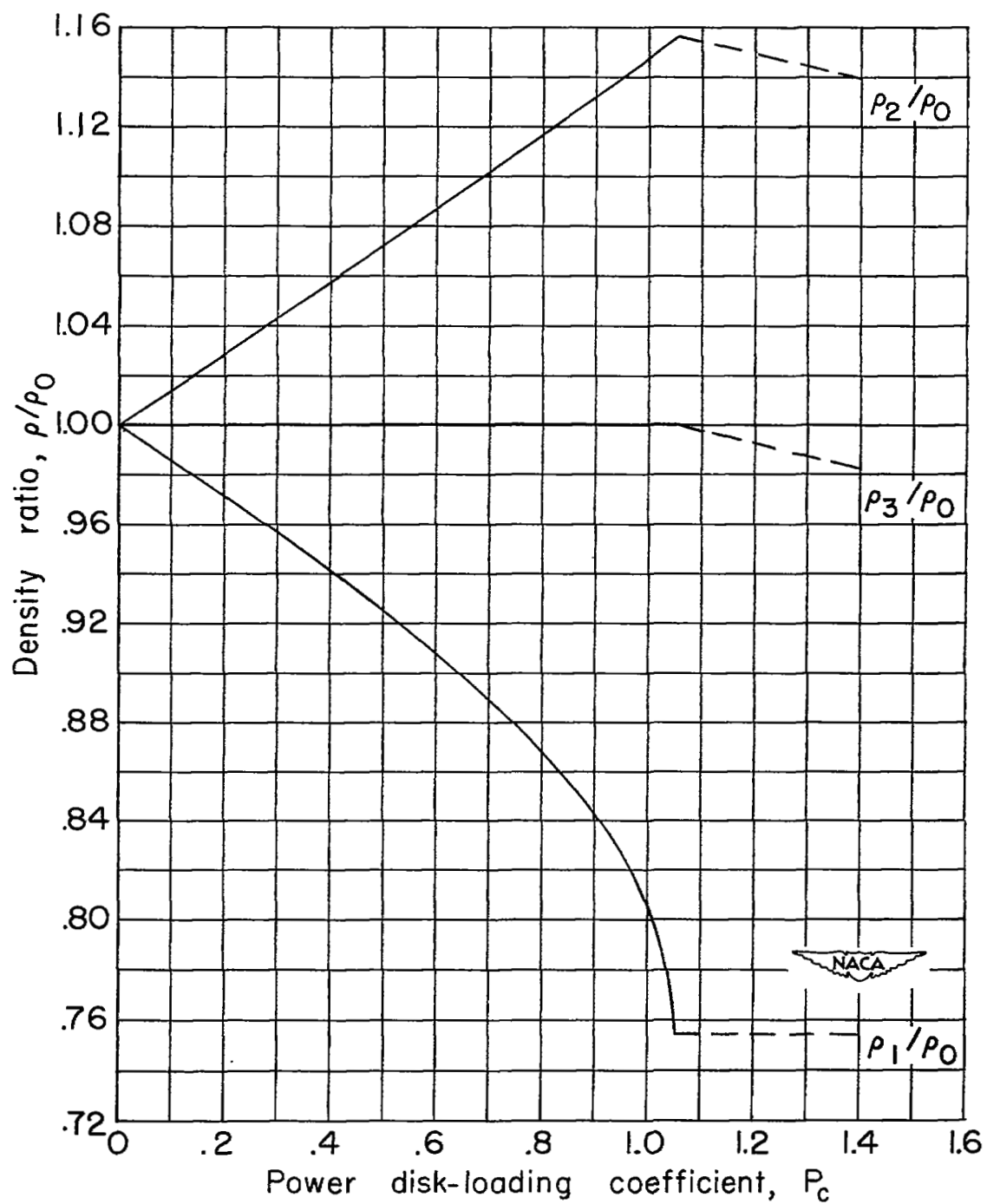
(b) Mach number.

Figure 3.- Continued.



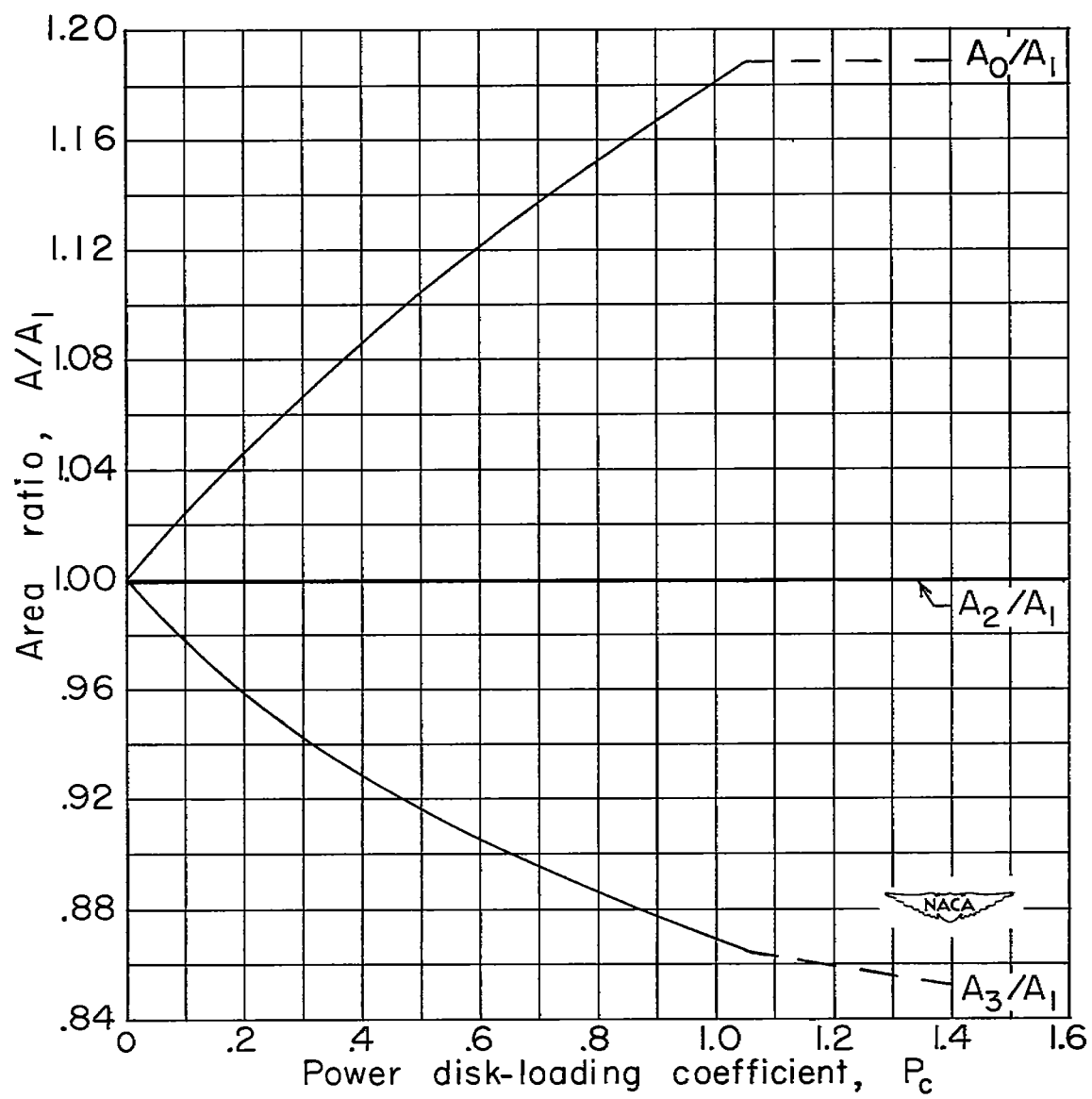
(c) Velocity ratio.

Figure 3.- Continued.



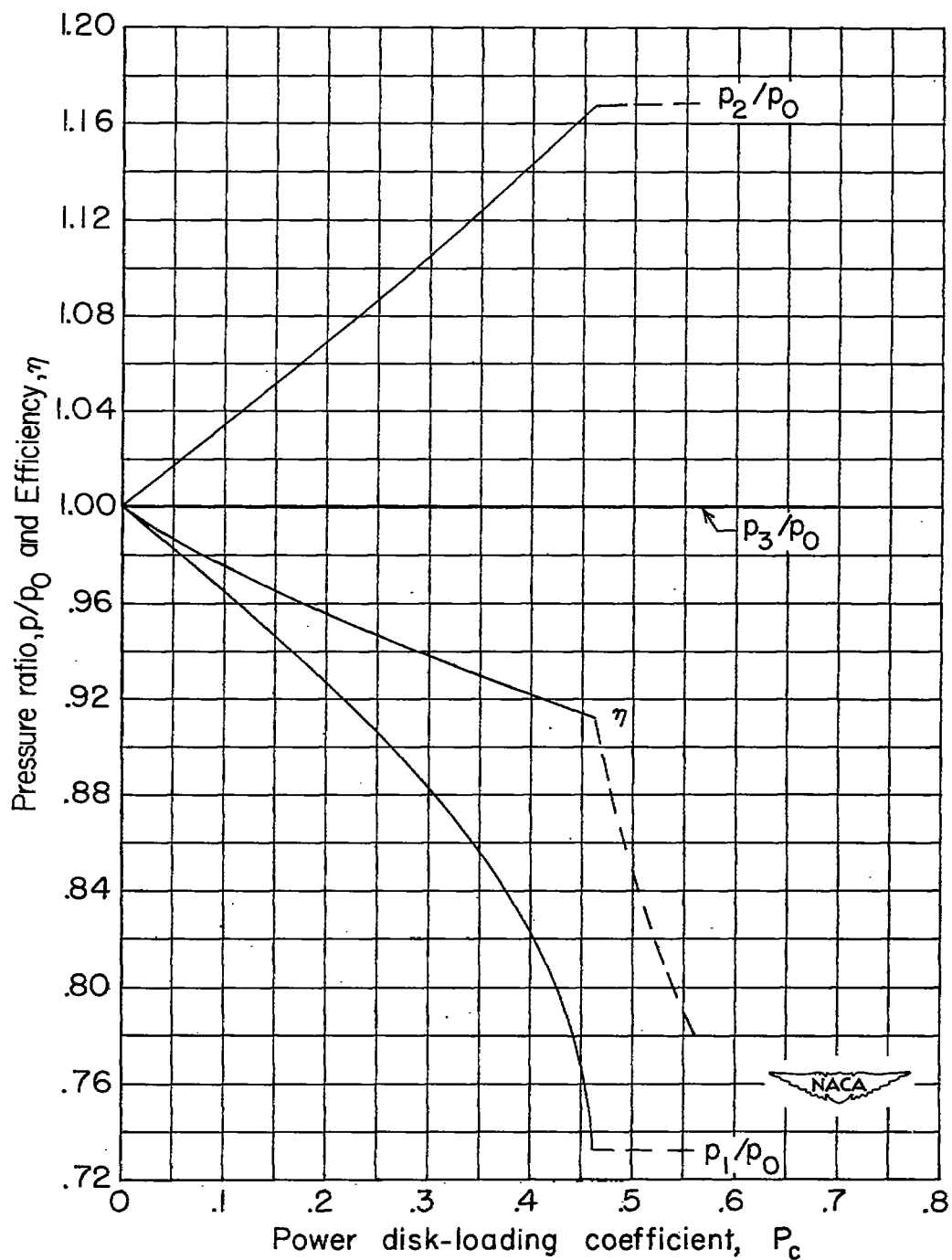
(d) Density ratio.

Figure 3.- Continued.



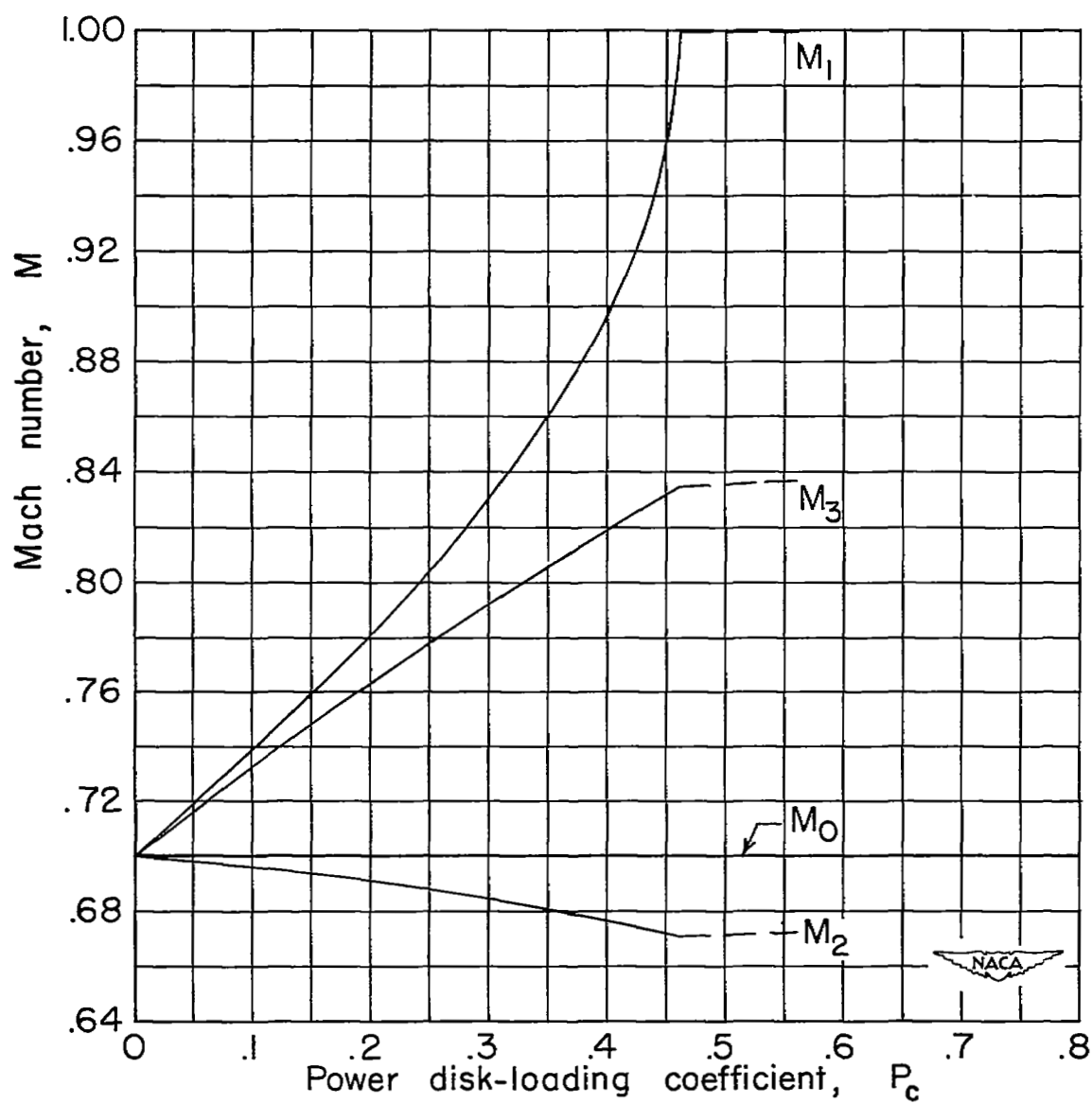
(e) Area ratio.

Figure 3.- Concluded.



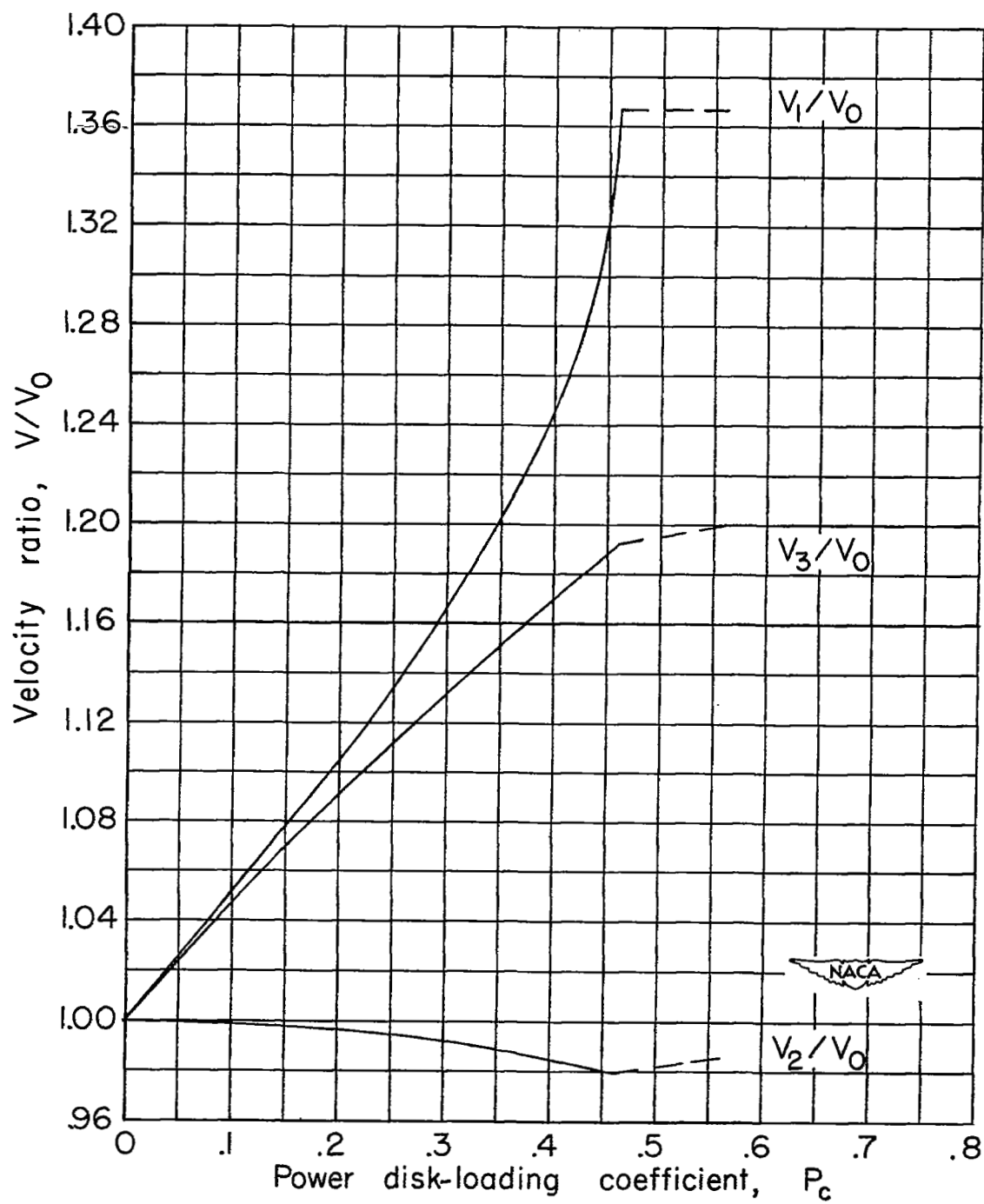
(a) Pressure ratio.

Figure 4.- Variation of slipstream flow factors with power loading.
 $M_0 = 0.70$.



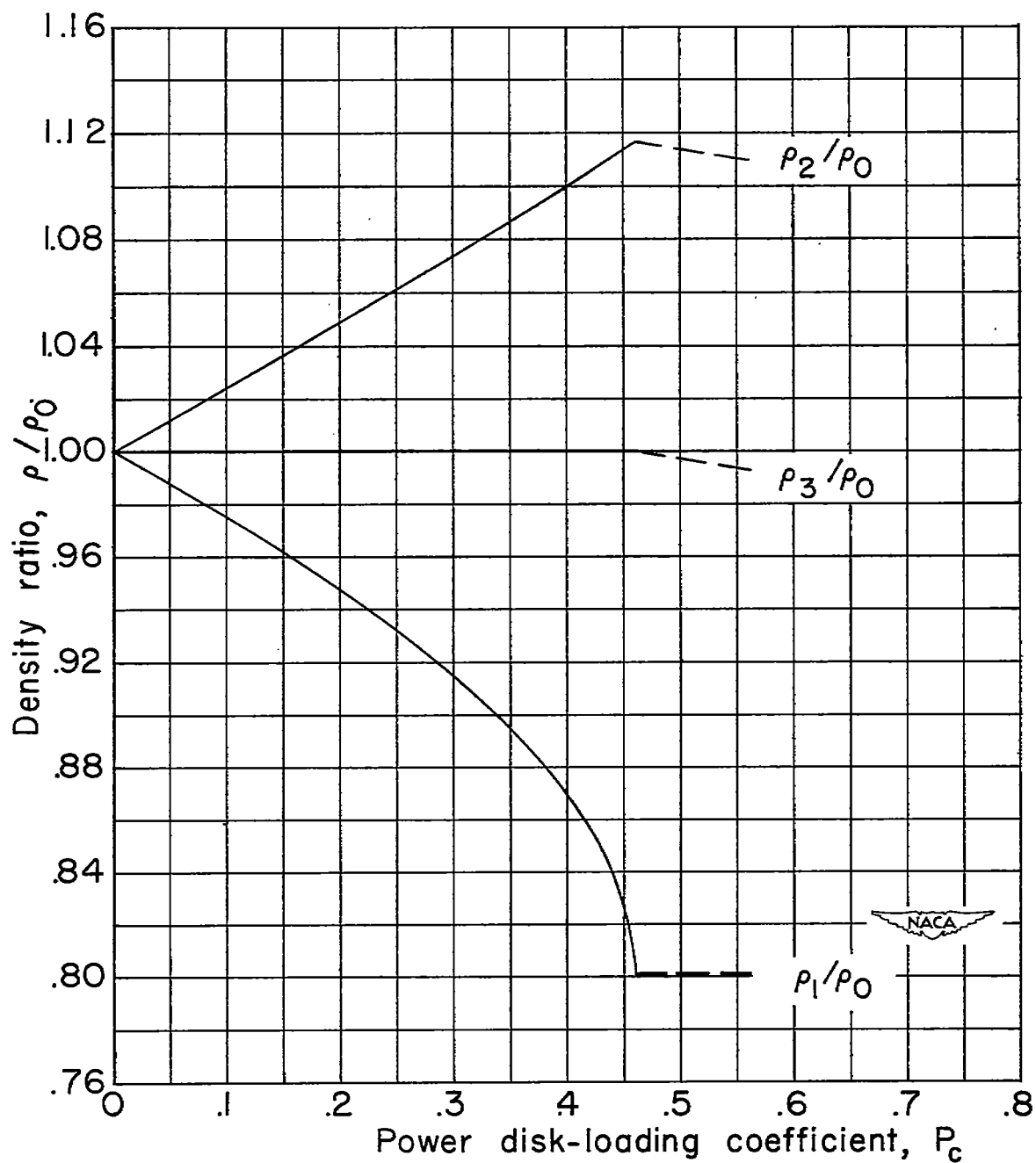
(b) Mach number.

Figure 4.- Continued.



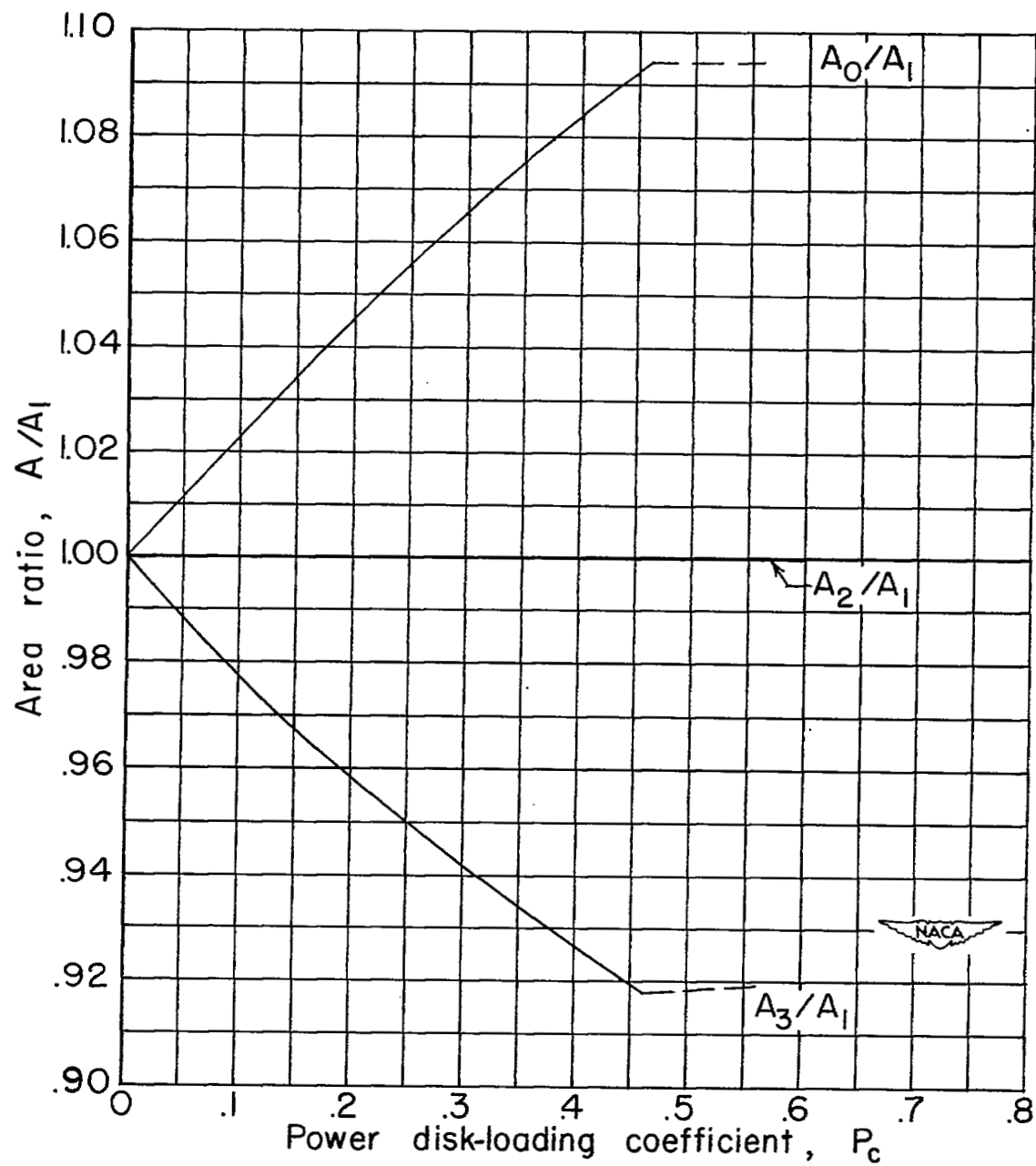
(c) Velocity ratio.

Figure 4.- Continued.



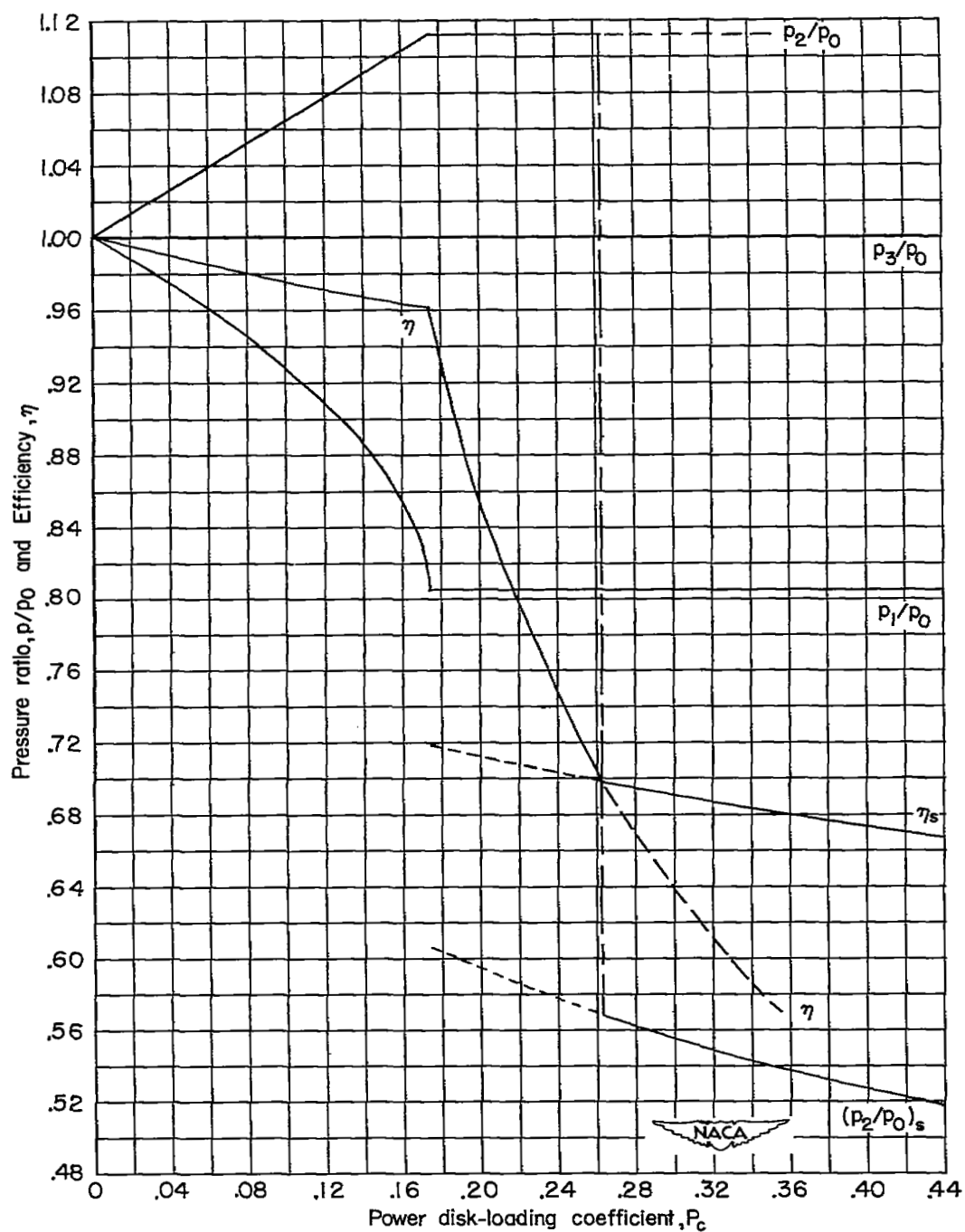
(d) Density ratio.

Figure 4.- Continued.



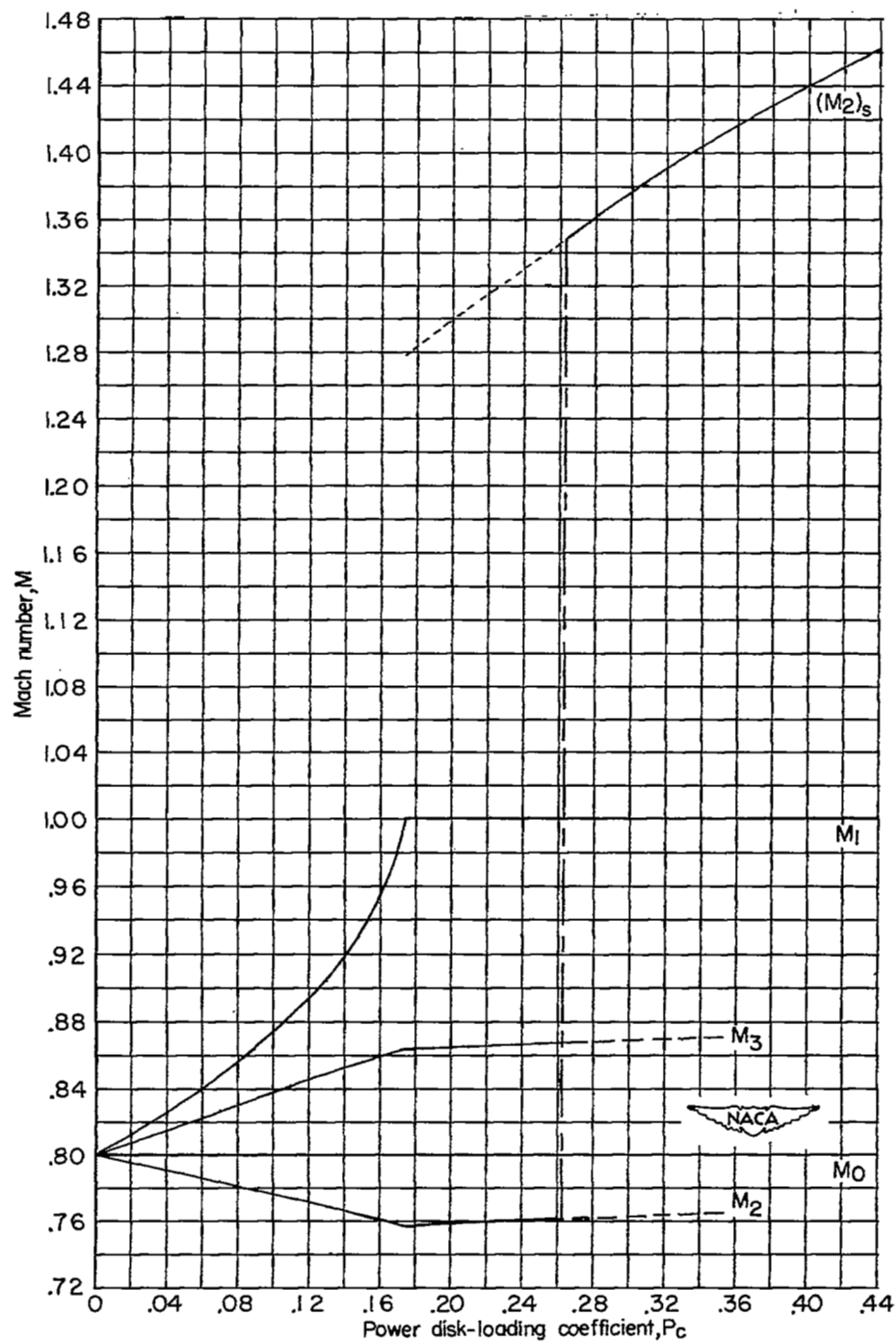
(e) Area ratio.

Figure 4.- Concluded.



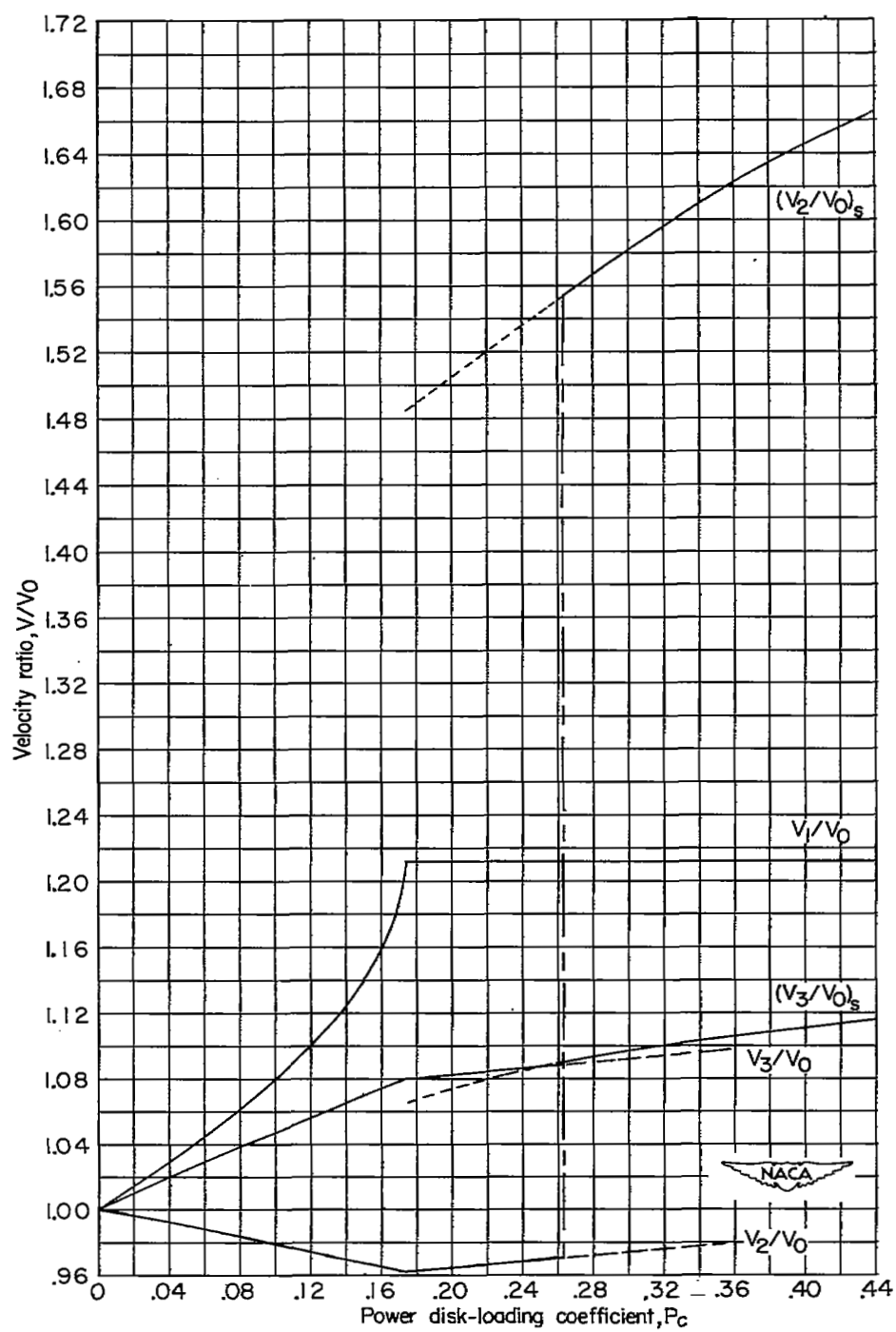
(a) Pressure ratio.

Figure 5.- Variation of slipstream flow factors with power loading.
 $M_0 = 0.80$.



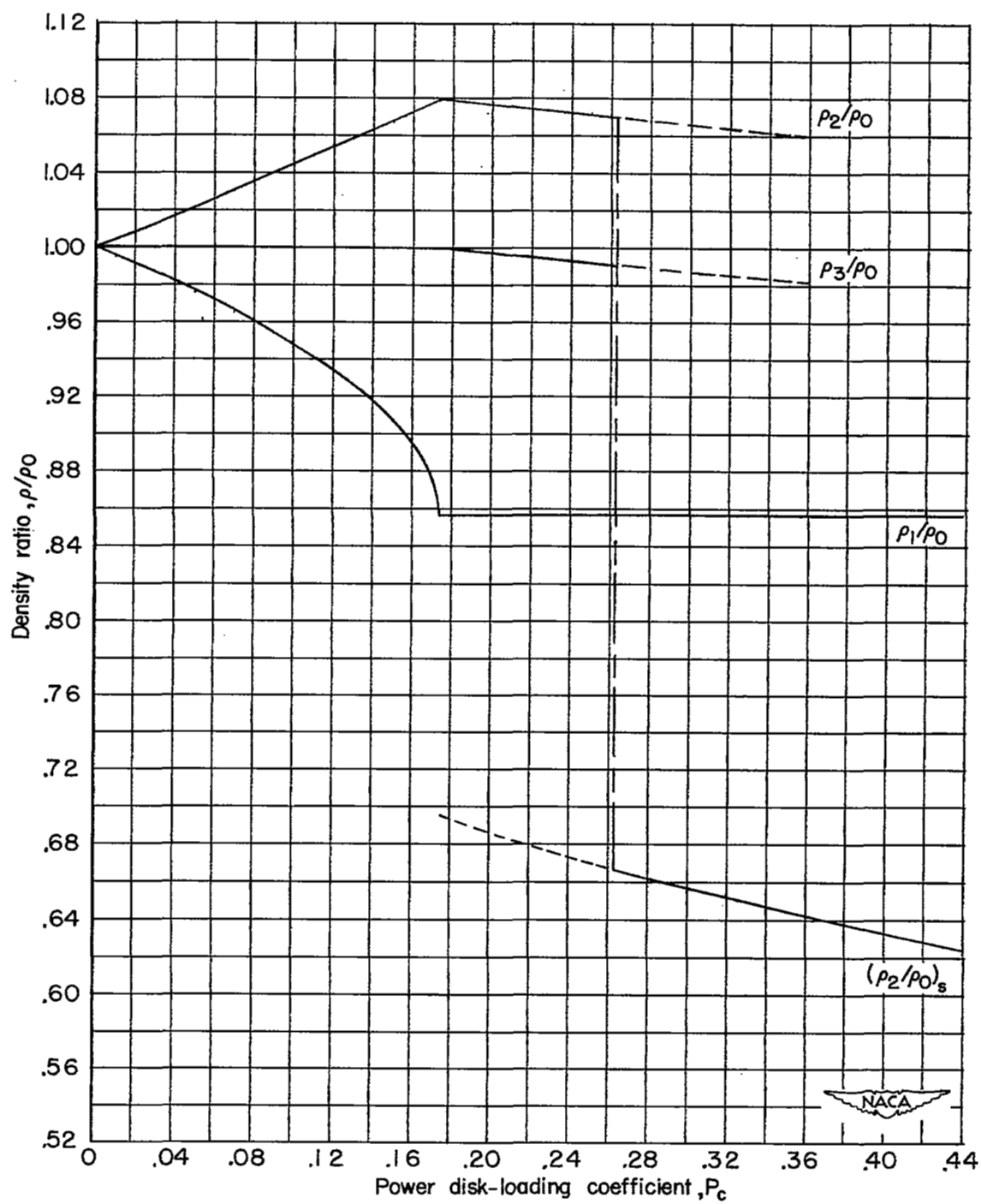
(b) Mach number.

Figure 5.- Continued.



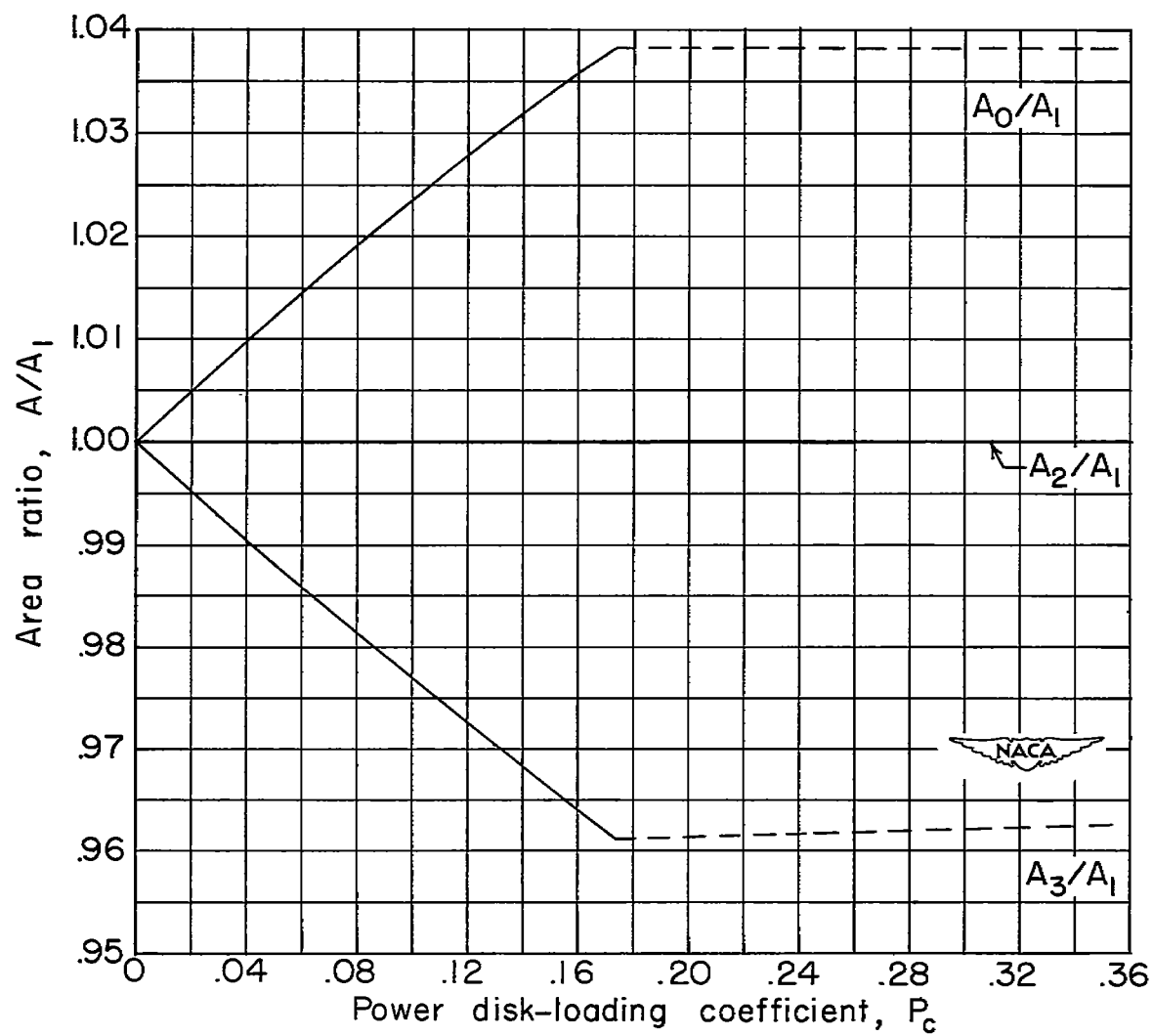
(c) Velocity ratio.

Figure 5.- Continued.



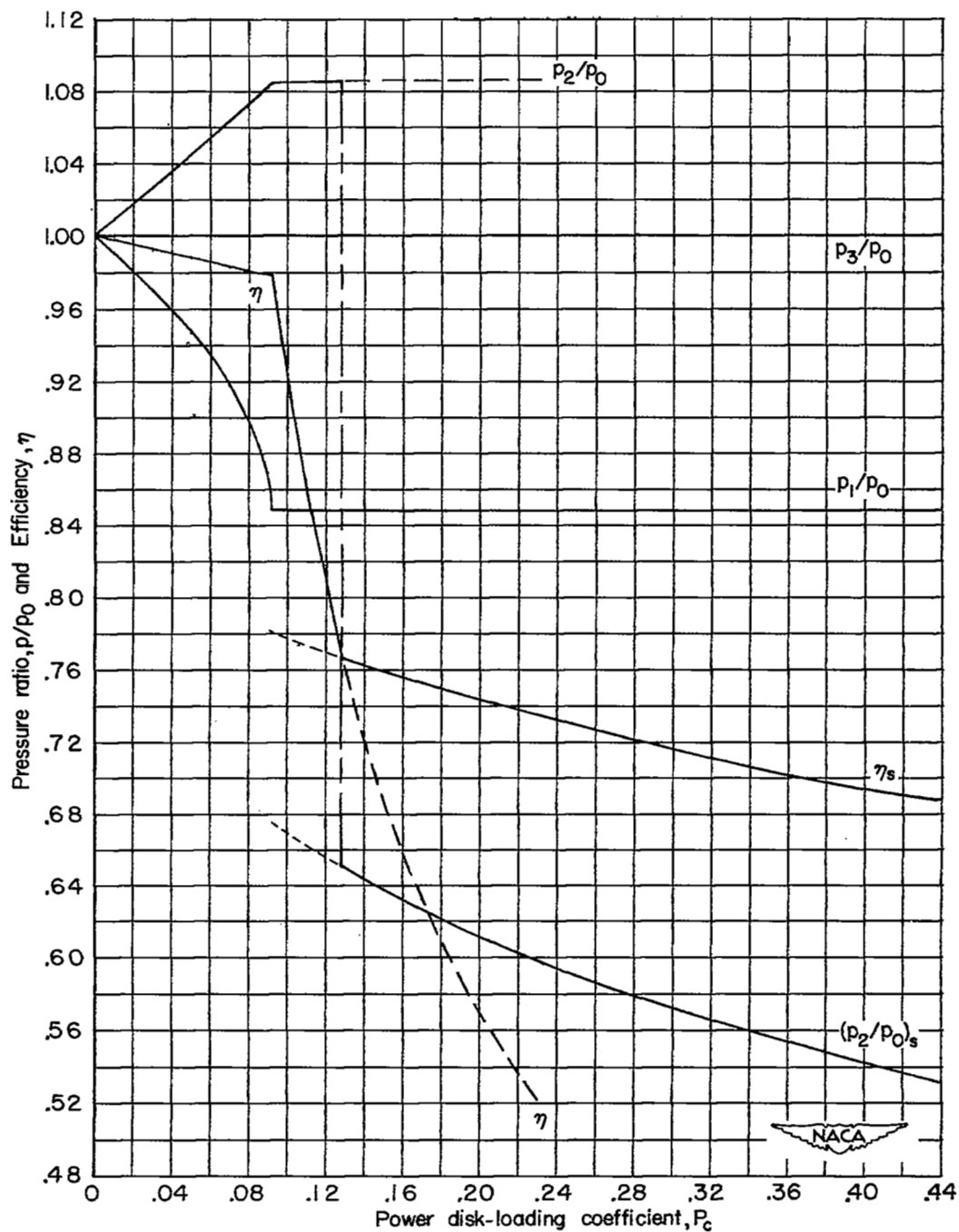
(d) Density ratio.

Figure 5.- Continued.



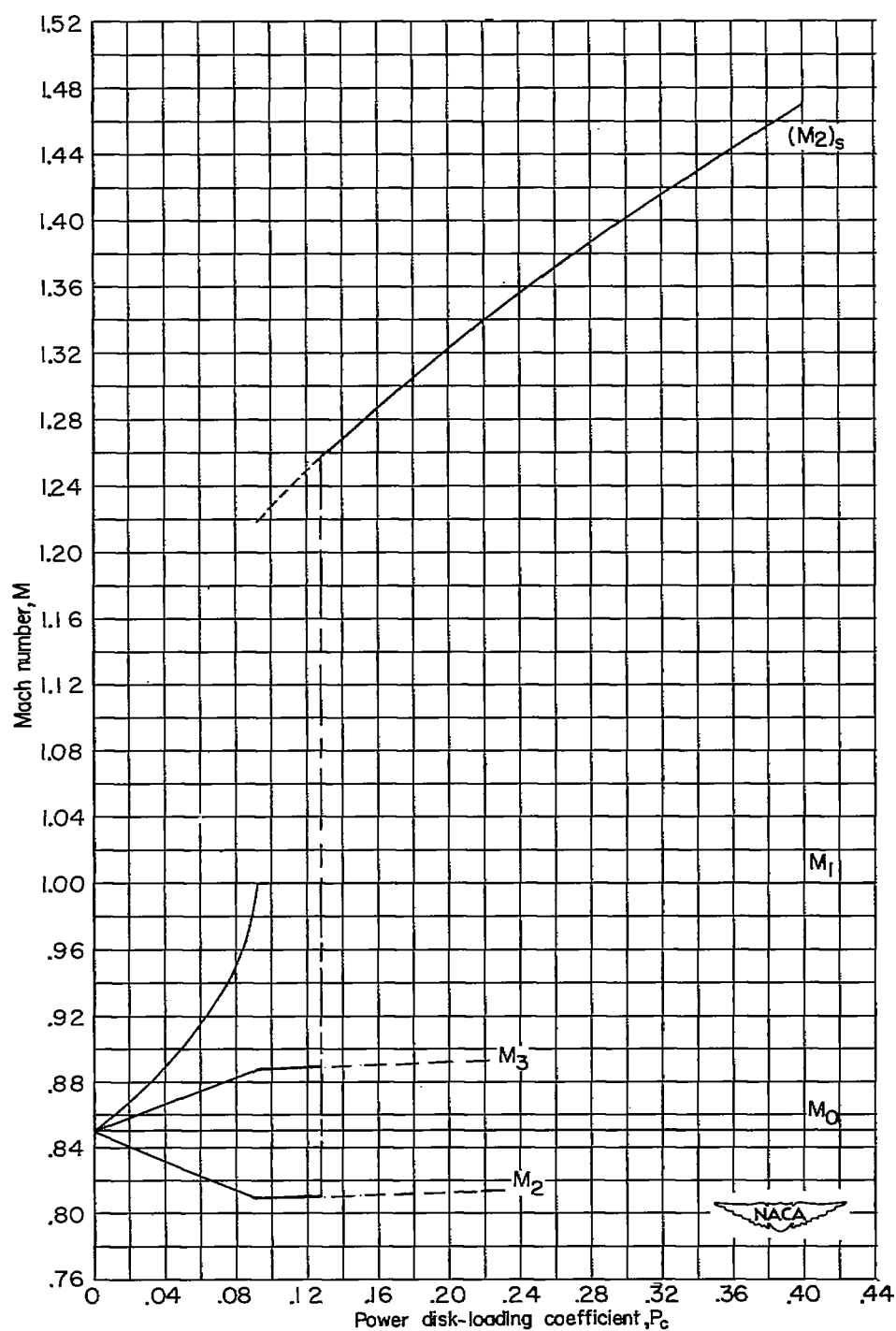
(e) Area ratio.

Figure 5.- Concluded.



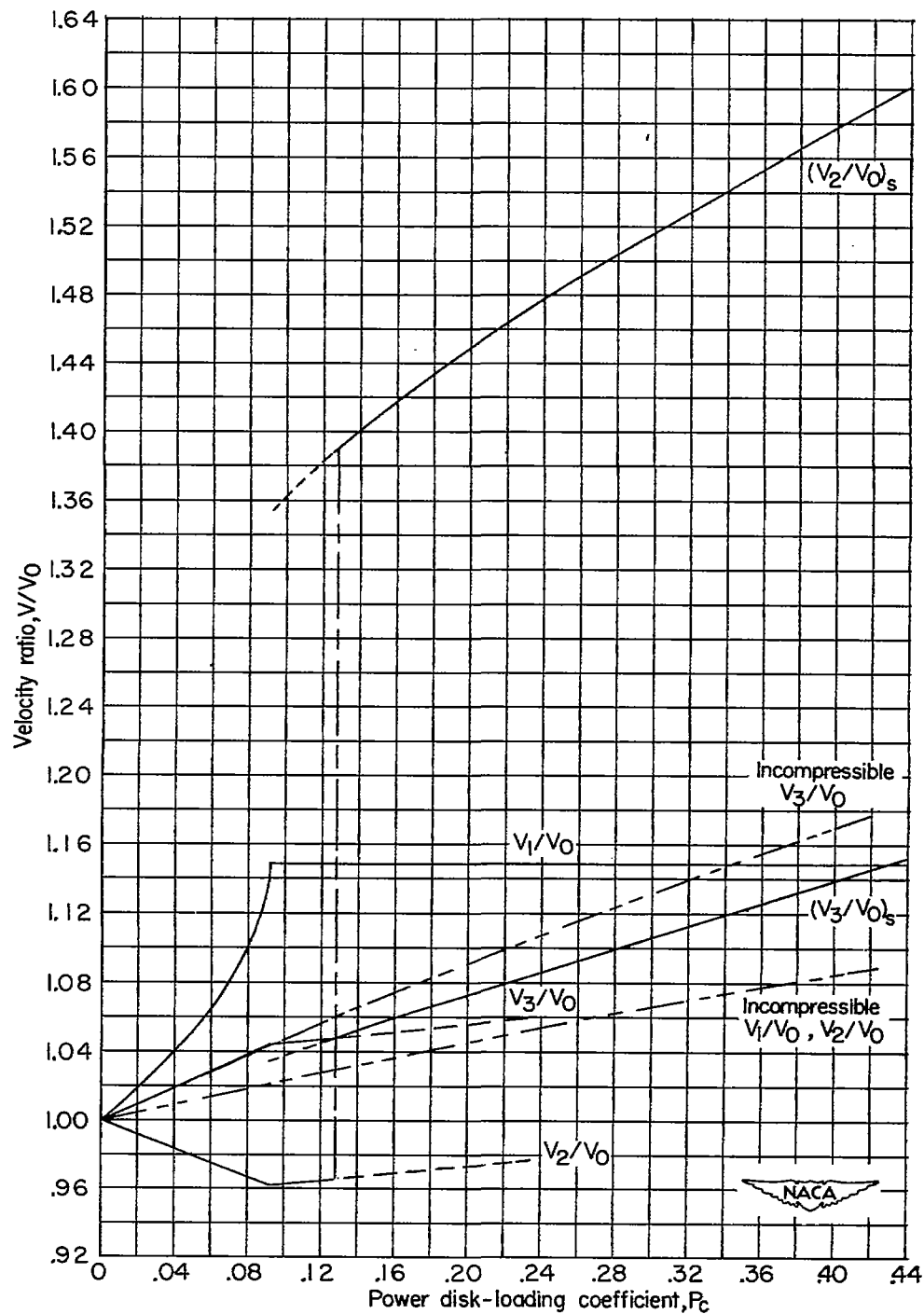
(a) Pressure ratio.

Figure 6.- Variation of slipstream flow factors with power loading.
 $M_0 = 0.85$.



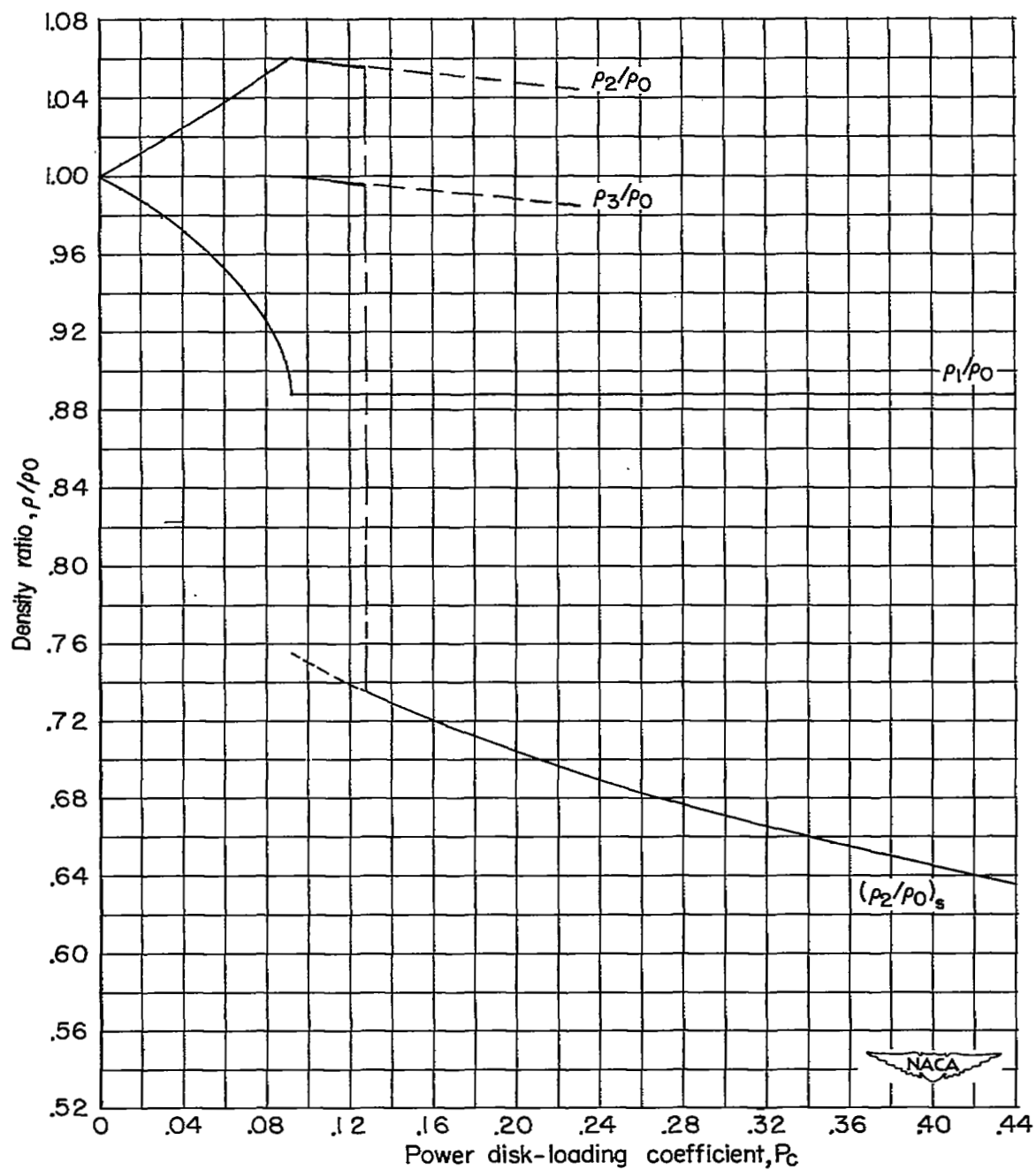
(b) Mach number.

Figure 6.- Continued.



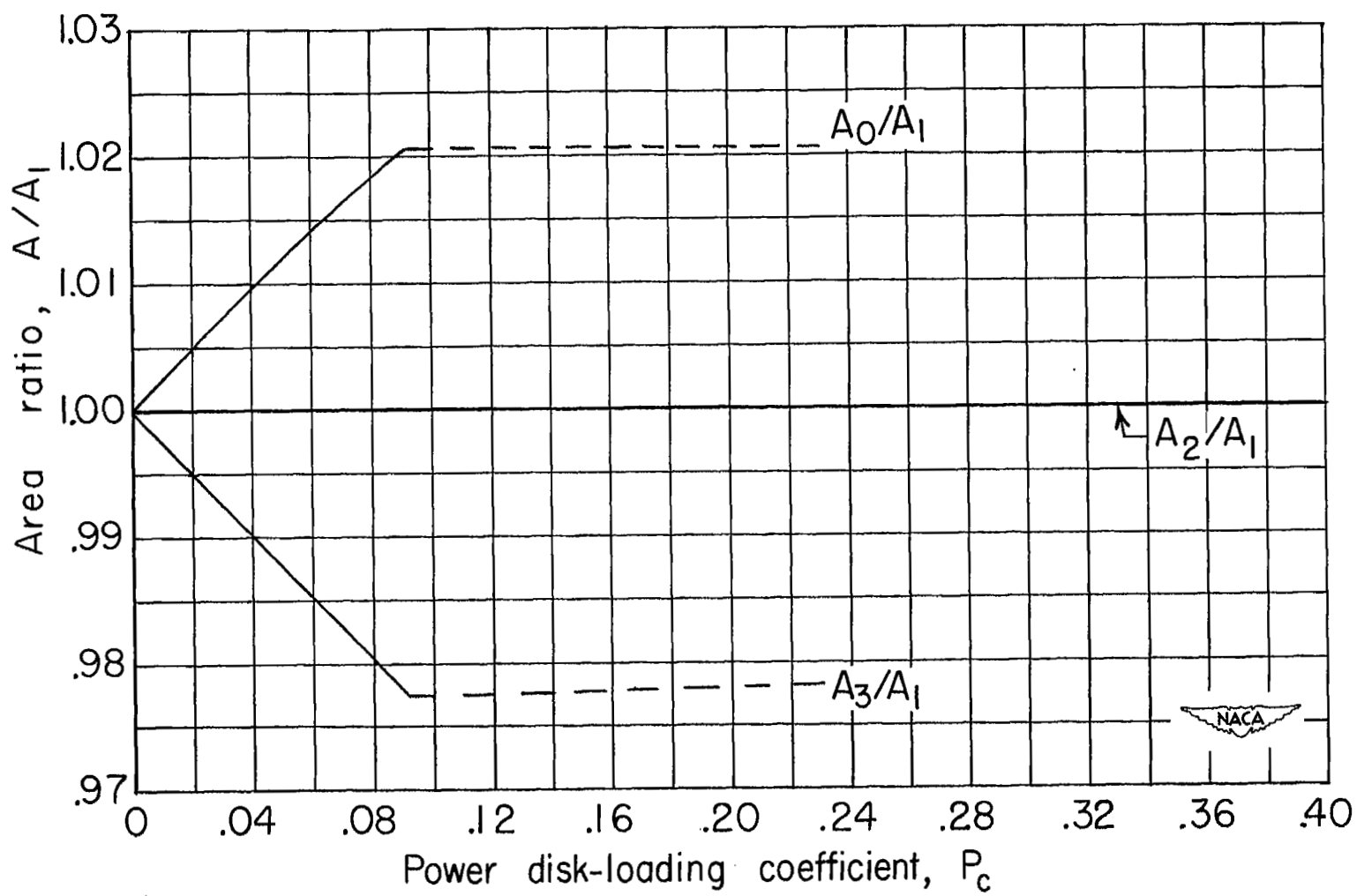
(c) Velocity ratio.

Figure 6.- Continued.



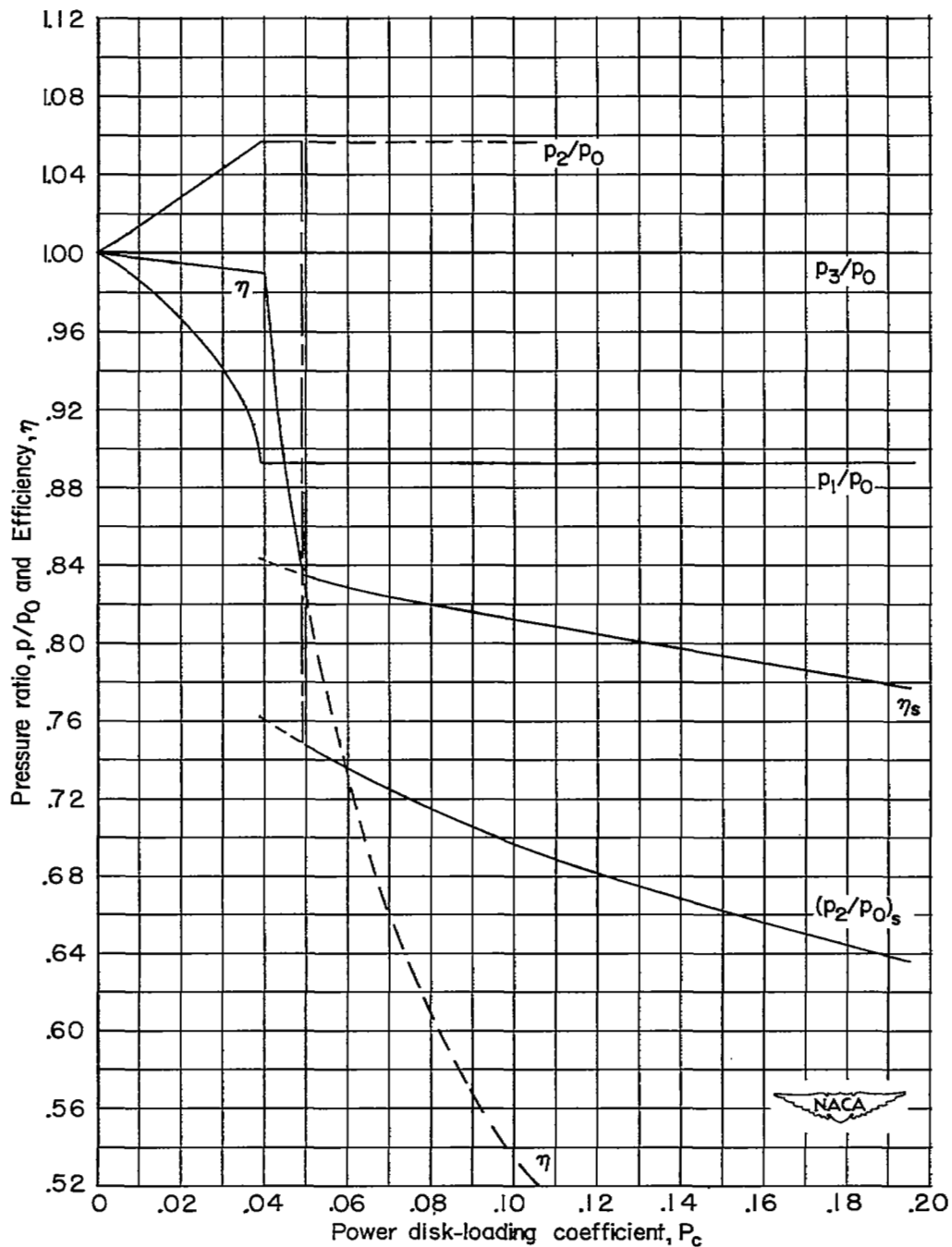
(d) Density ratio.

Figure 6.- Continued.



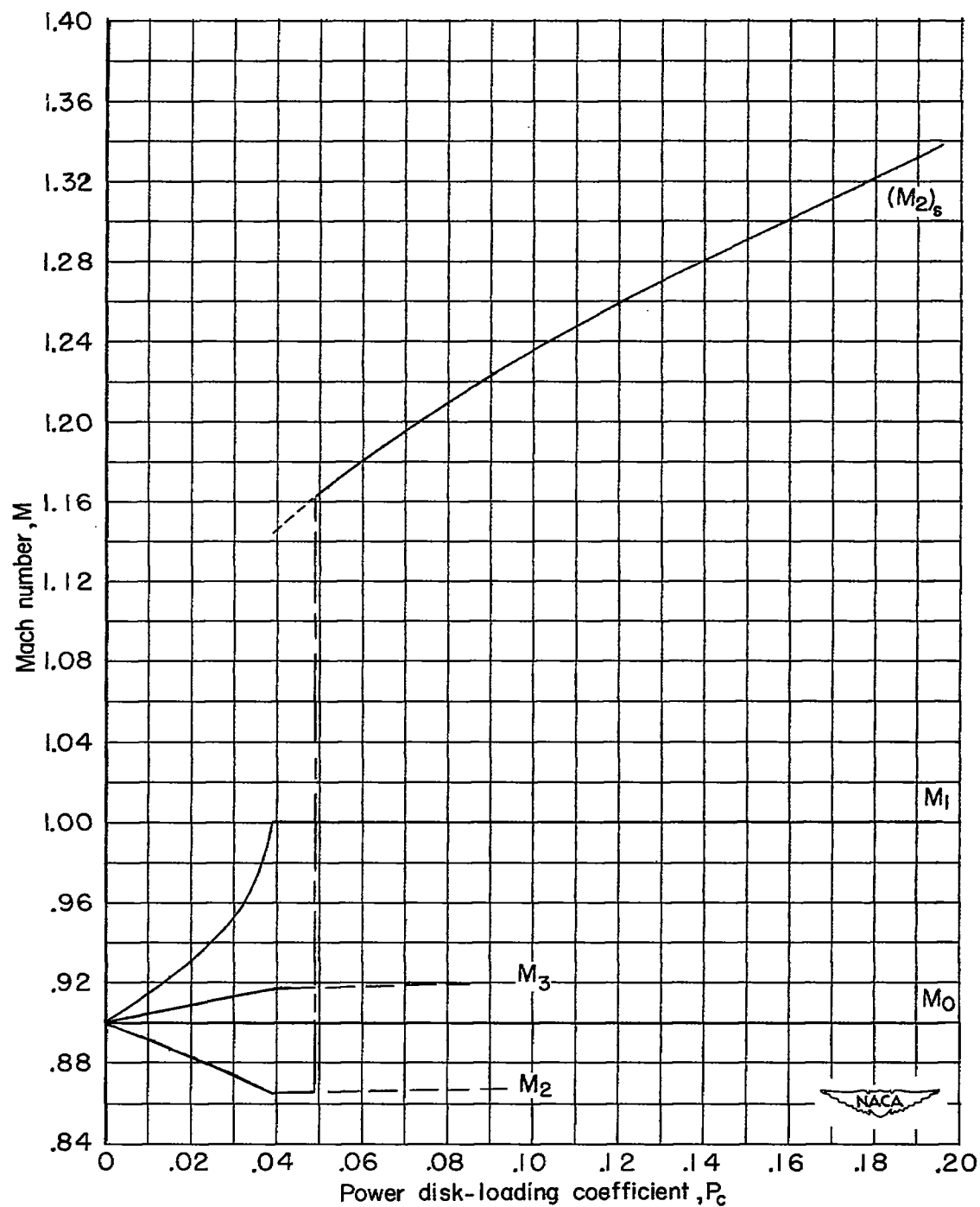
(e) Area ratio.

Figure 6.- Concluded.



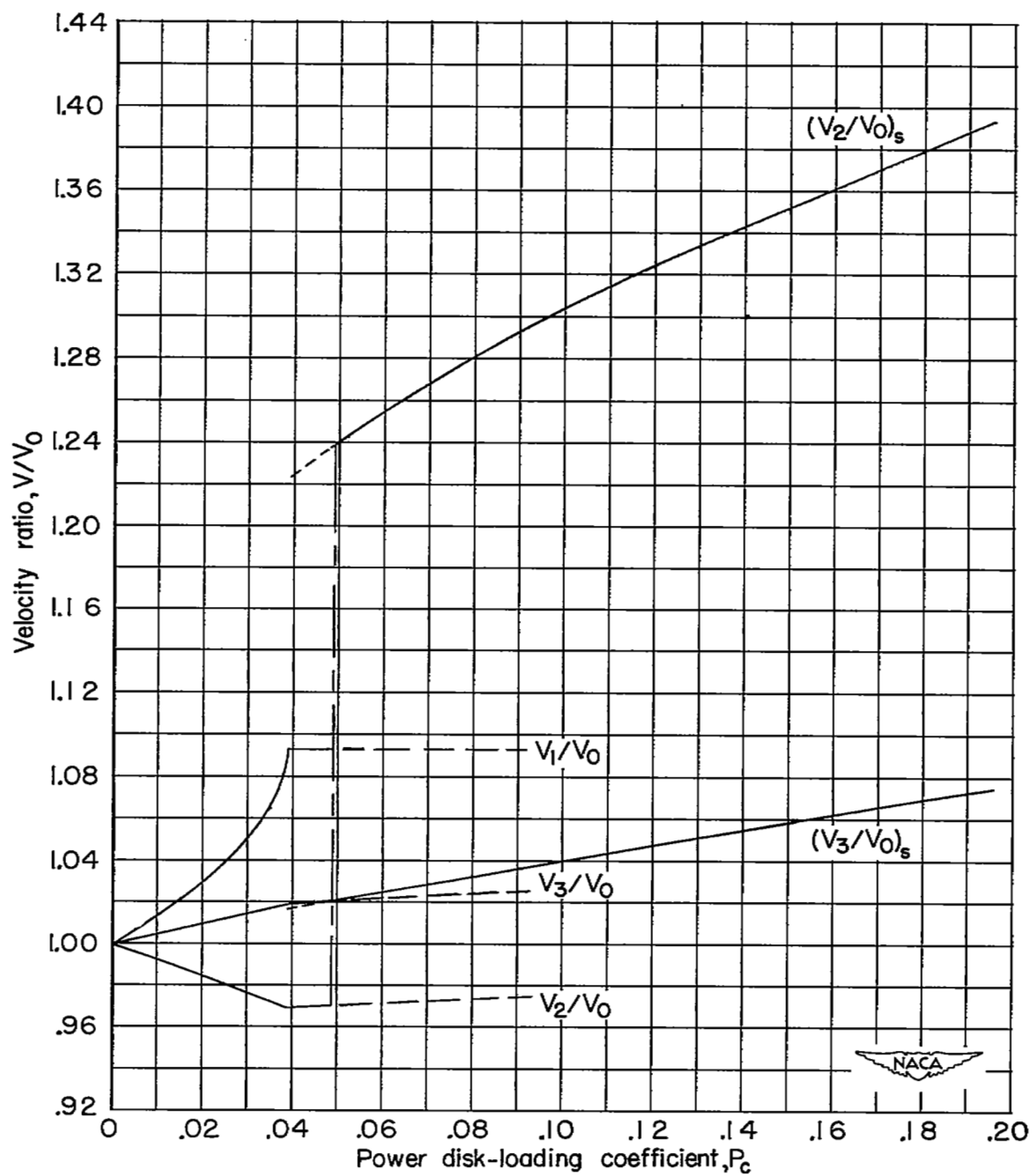
(a) Pressure ratio.

Figure 7.- Variation of slipstream flow factors with power loading.
 $M_0 = 0.90$.



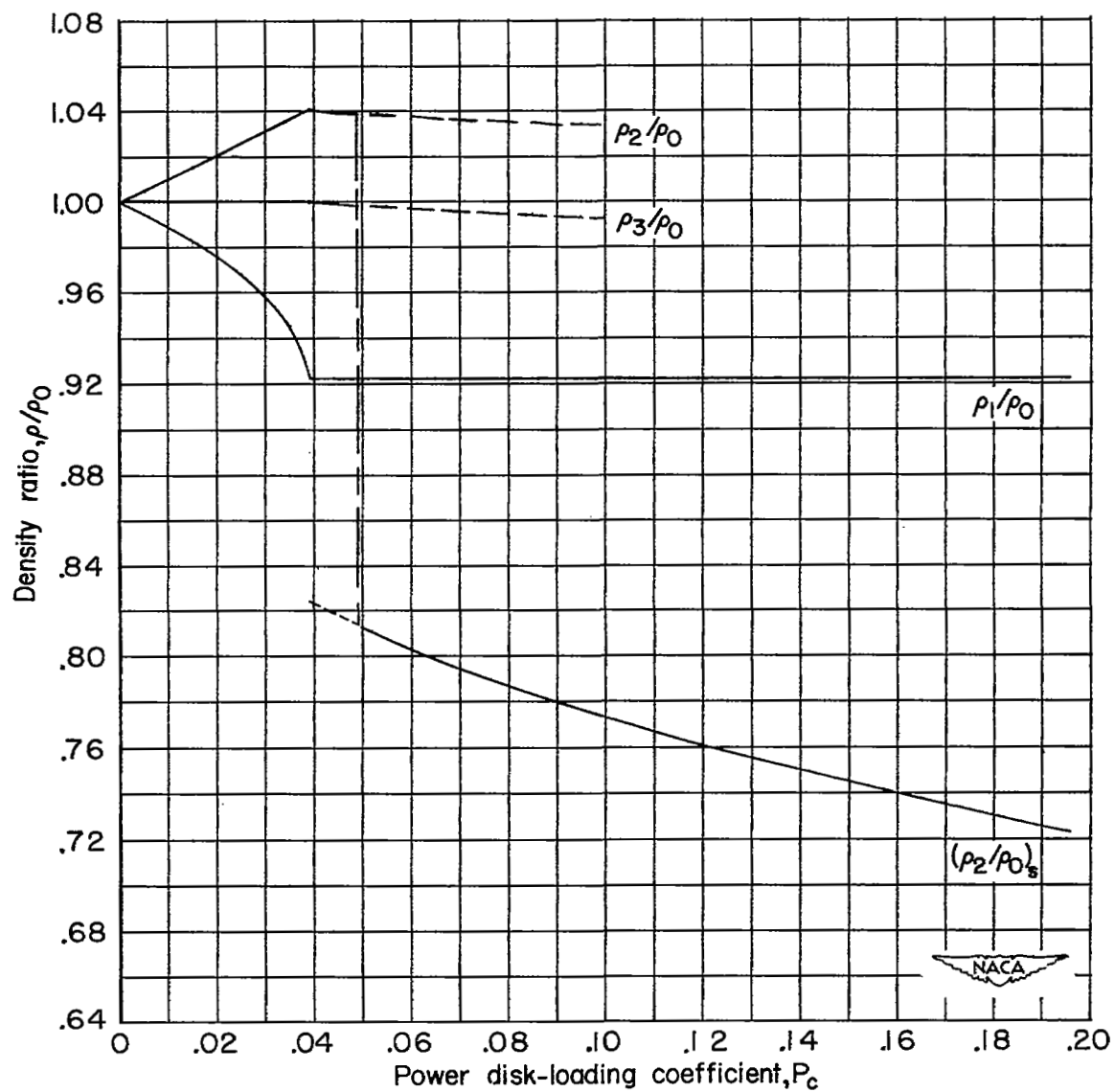
(b) Mach number.

Figure 7.- Continued.



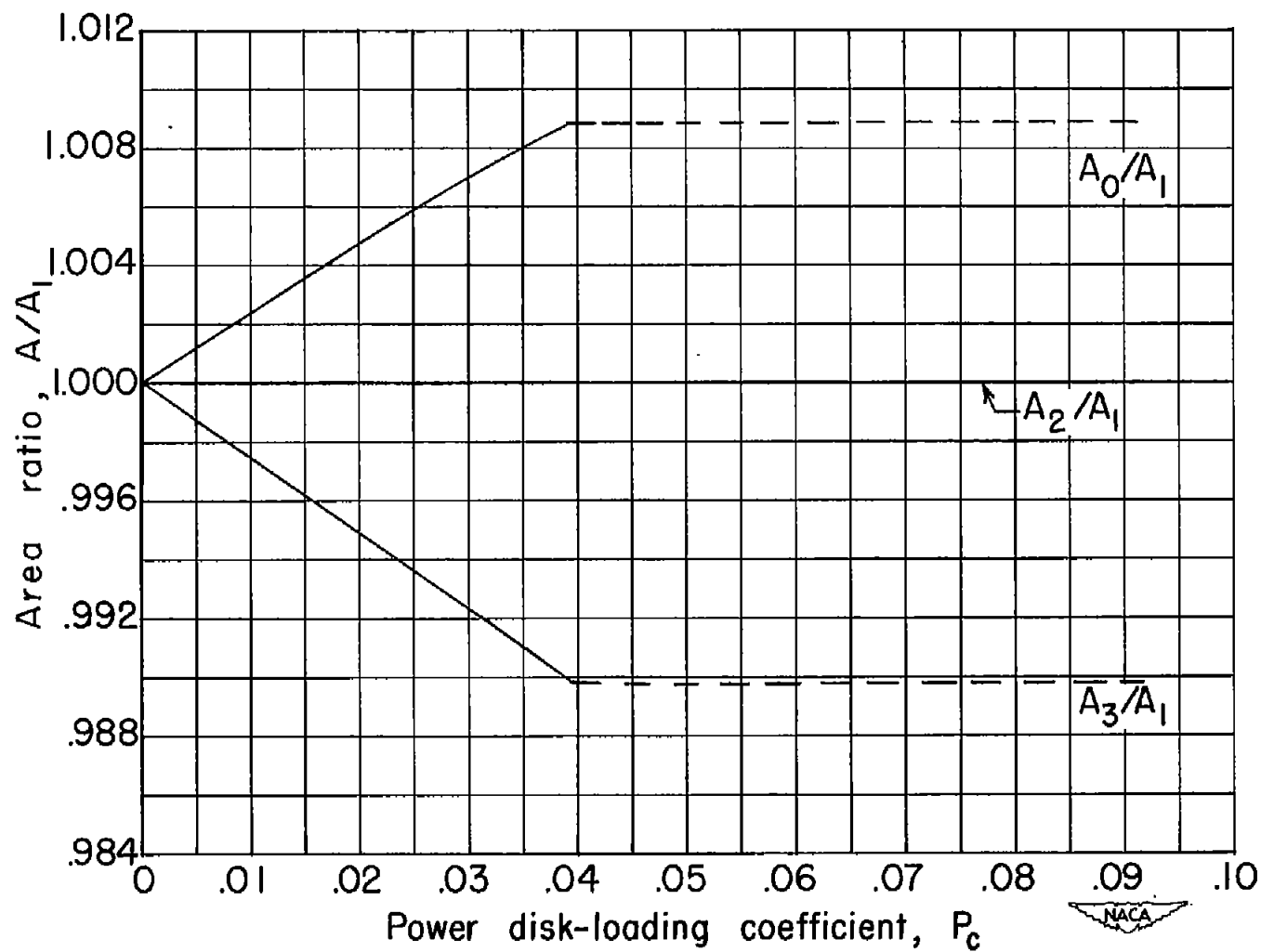
(c) Velocity ratio.

Figure 7.- Continued.



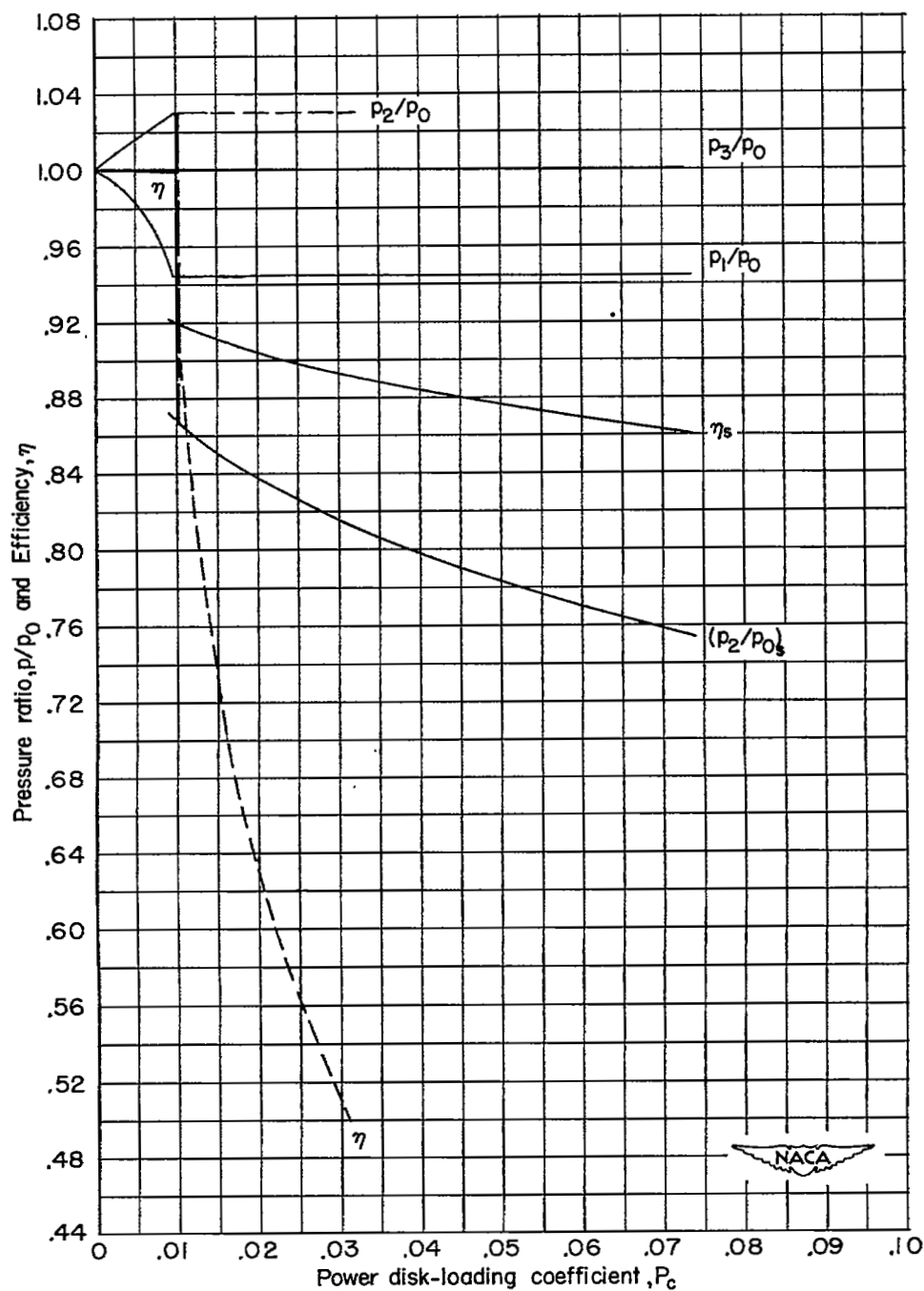
(d) Density ratio.

Figure 7.- Continued.



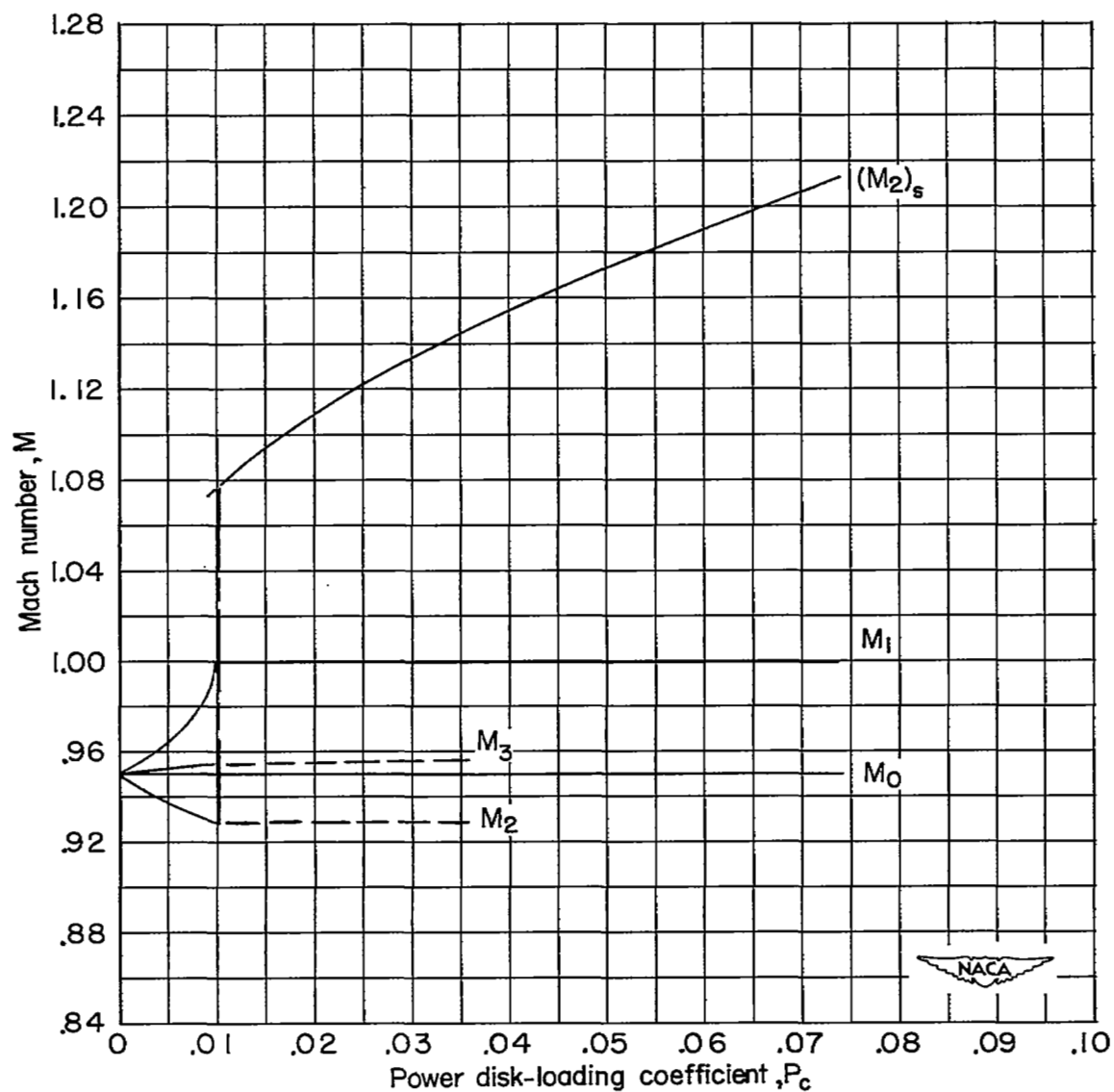
(e) Area ratio.

Figure 7.- Concluded.



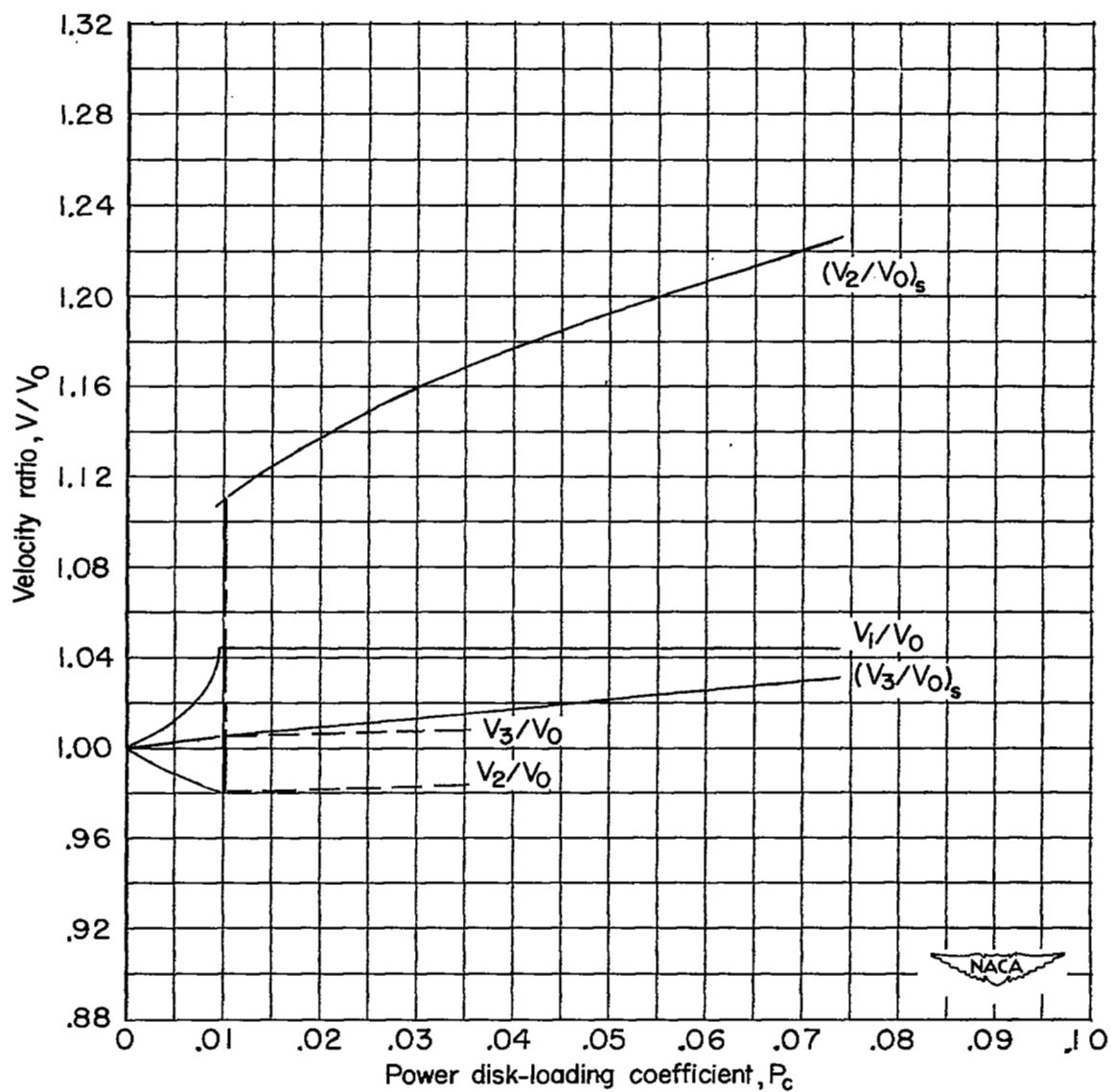
(a) Pressure ratio.

Figure 8.- Variation of slipstream flow factors with power loading.
 $M_0 = 0.95$.



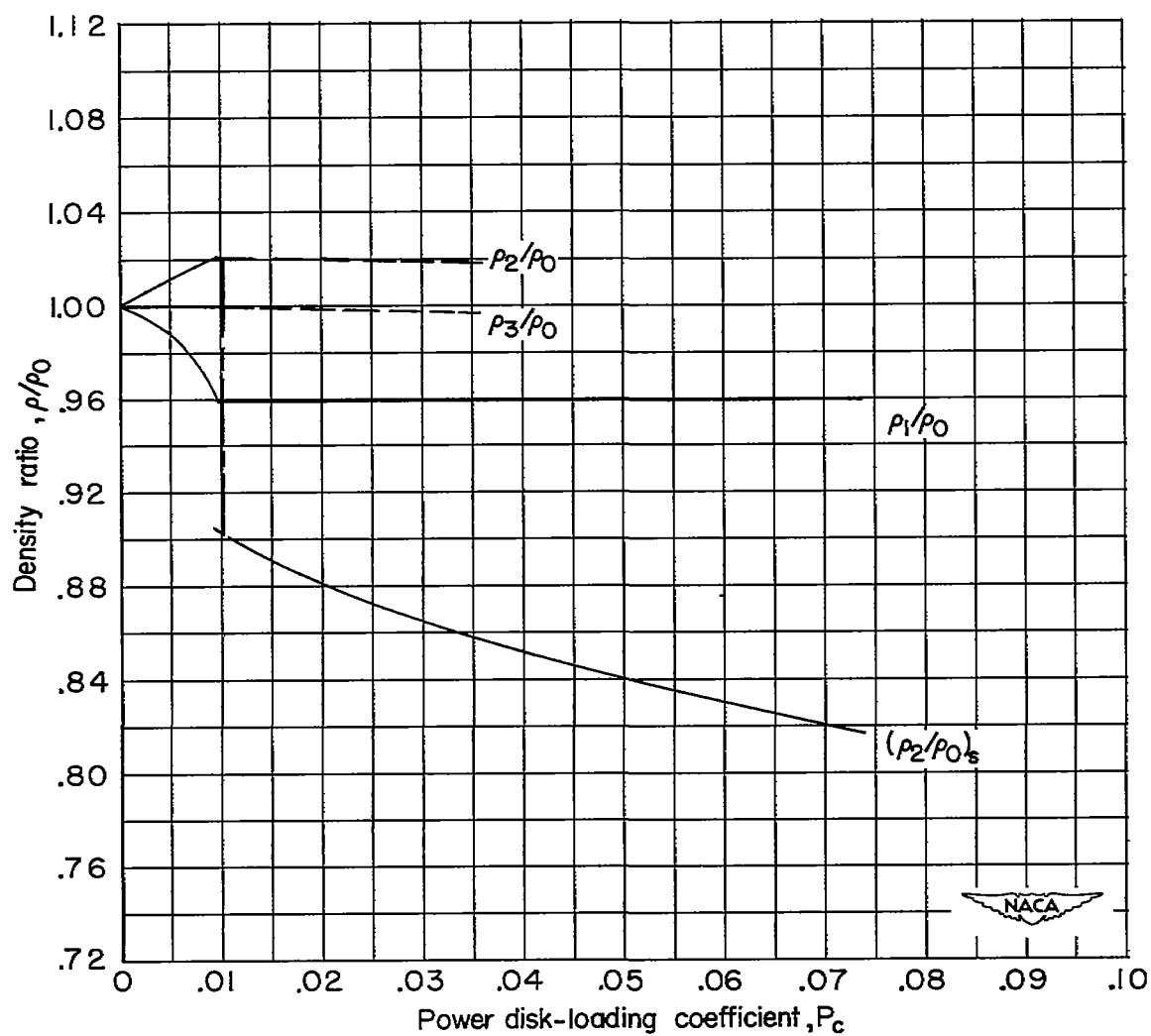
(b) Mach number.

Figure 8.- Continued.



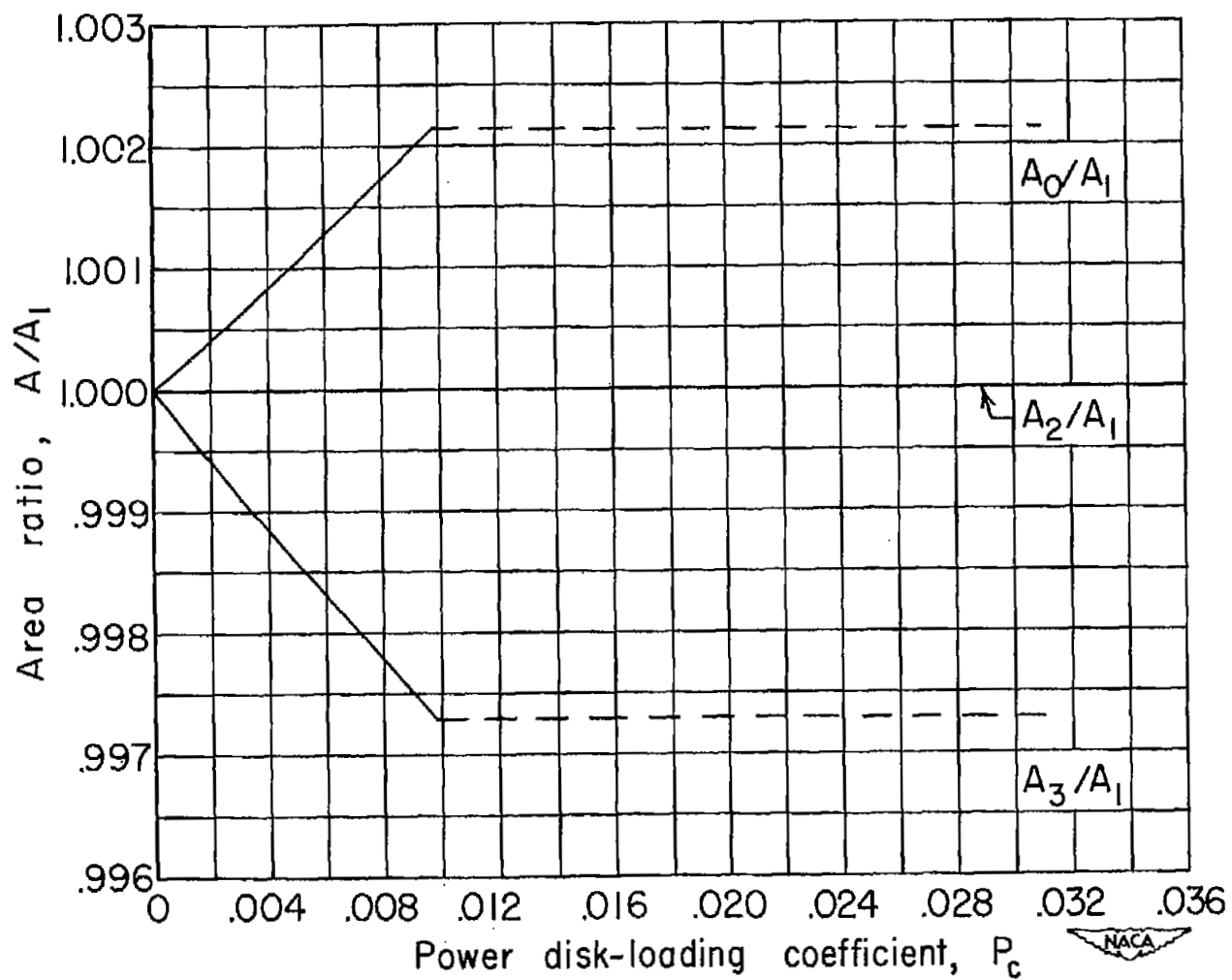
(c) Velocity ratio.

Figure 8.- Continued.



(d) Density ratio.

Figure 8.- Continued.



(e) Area ratio.

Figure 8.- Concluded.

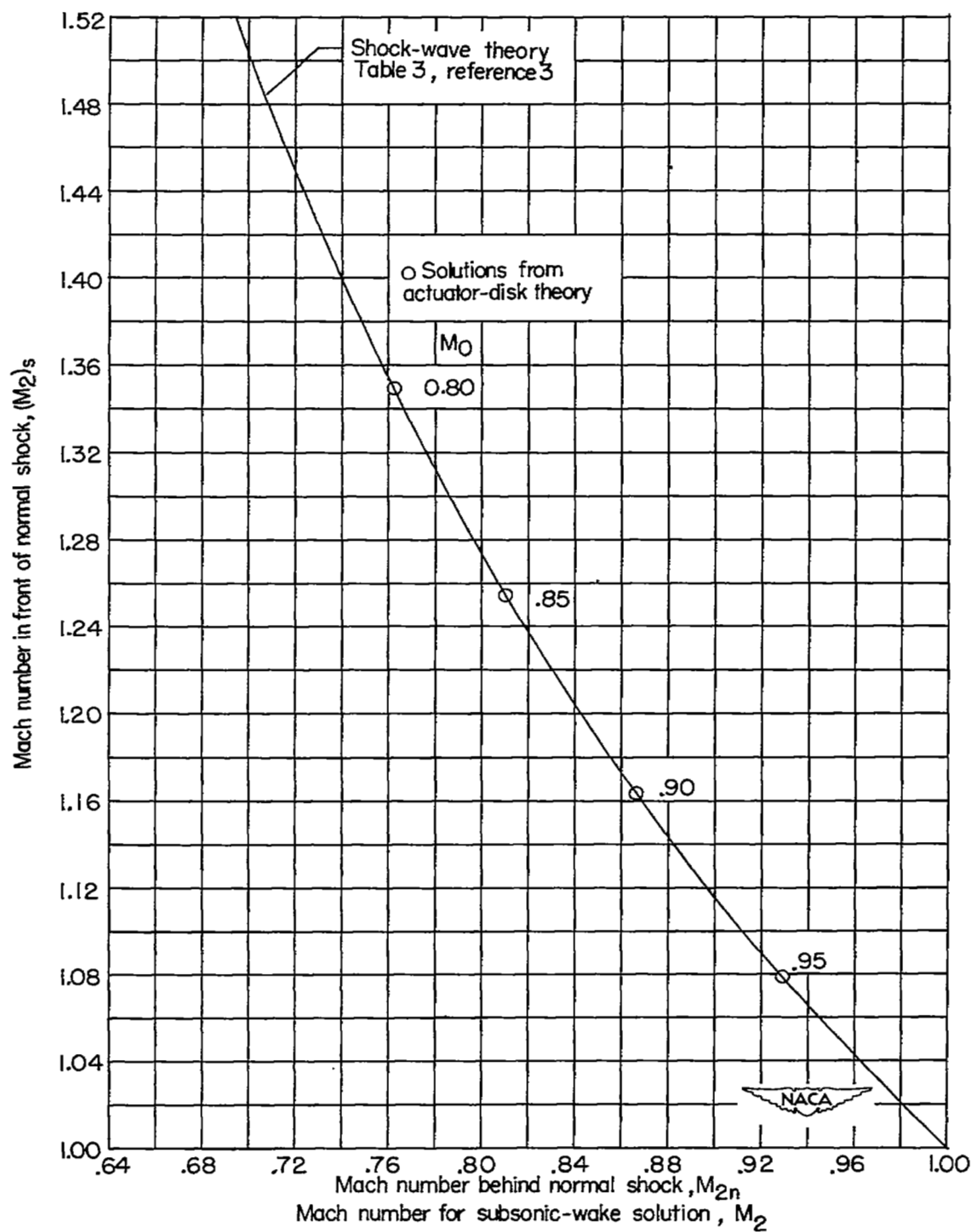


Figure 9.- Mach number relation for normal shock and correlation with solutions from actuator-disk theory.

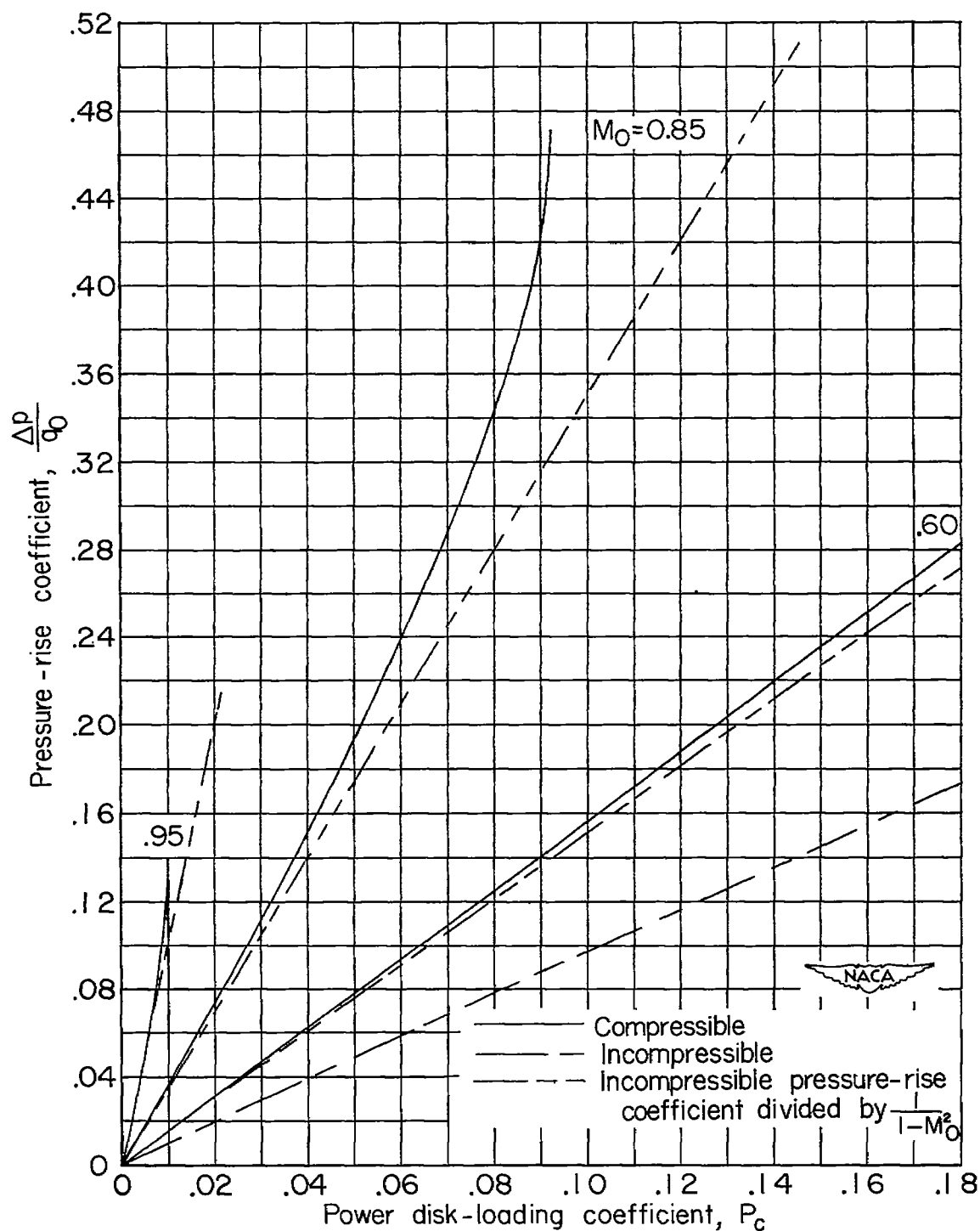


Figure 10.- Disk pressure-rise coefficient for incompressible and unchoked compressible flows.

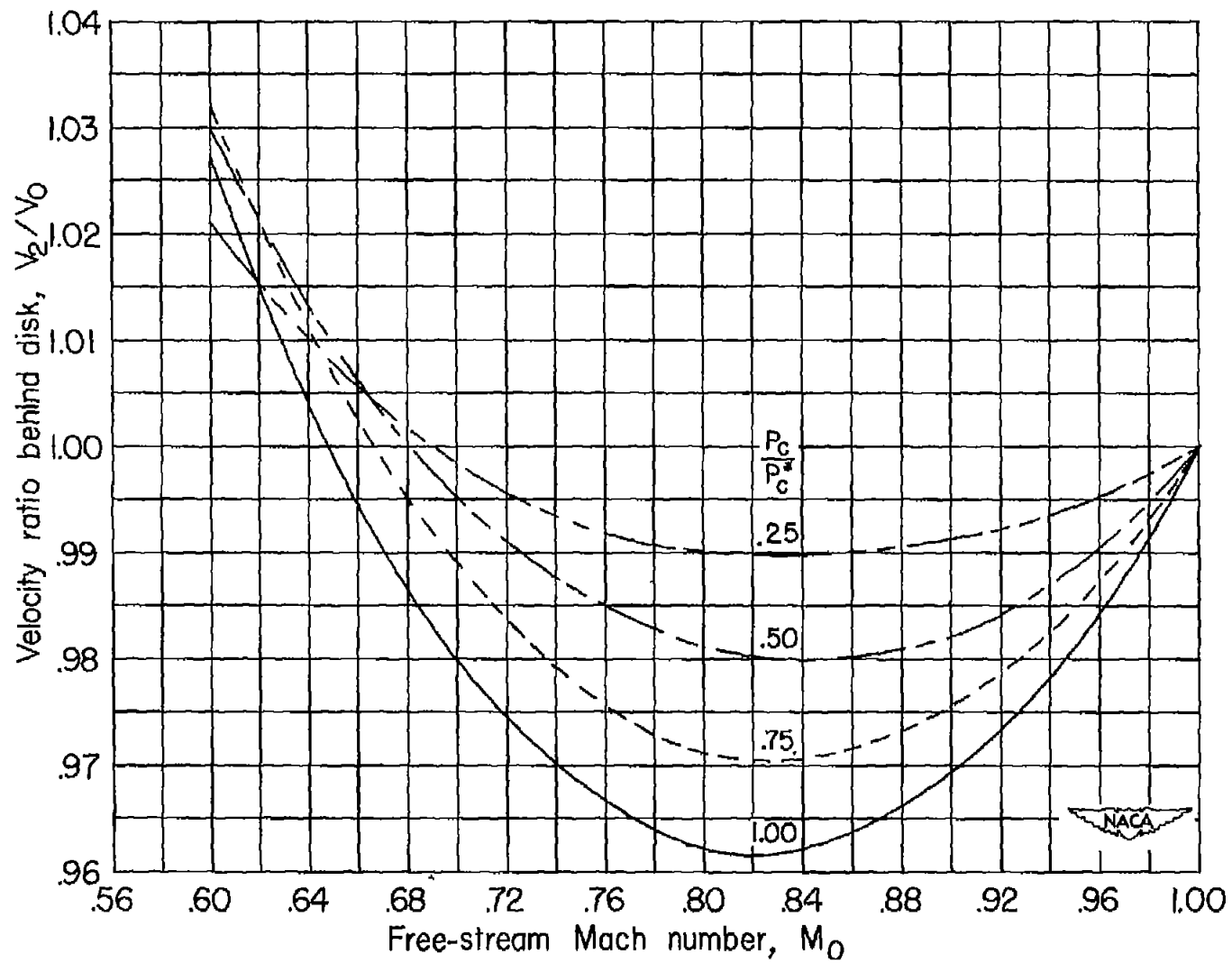
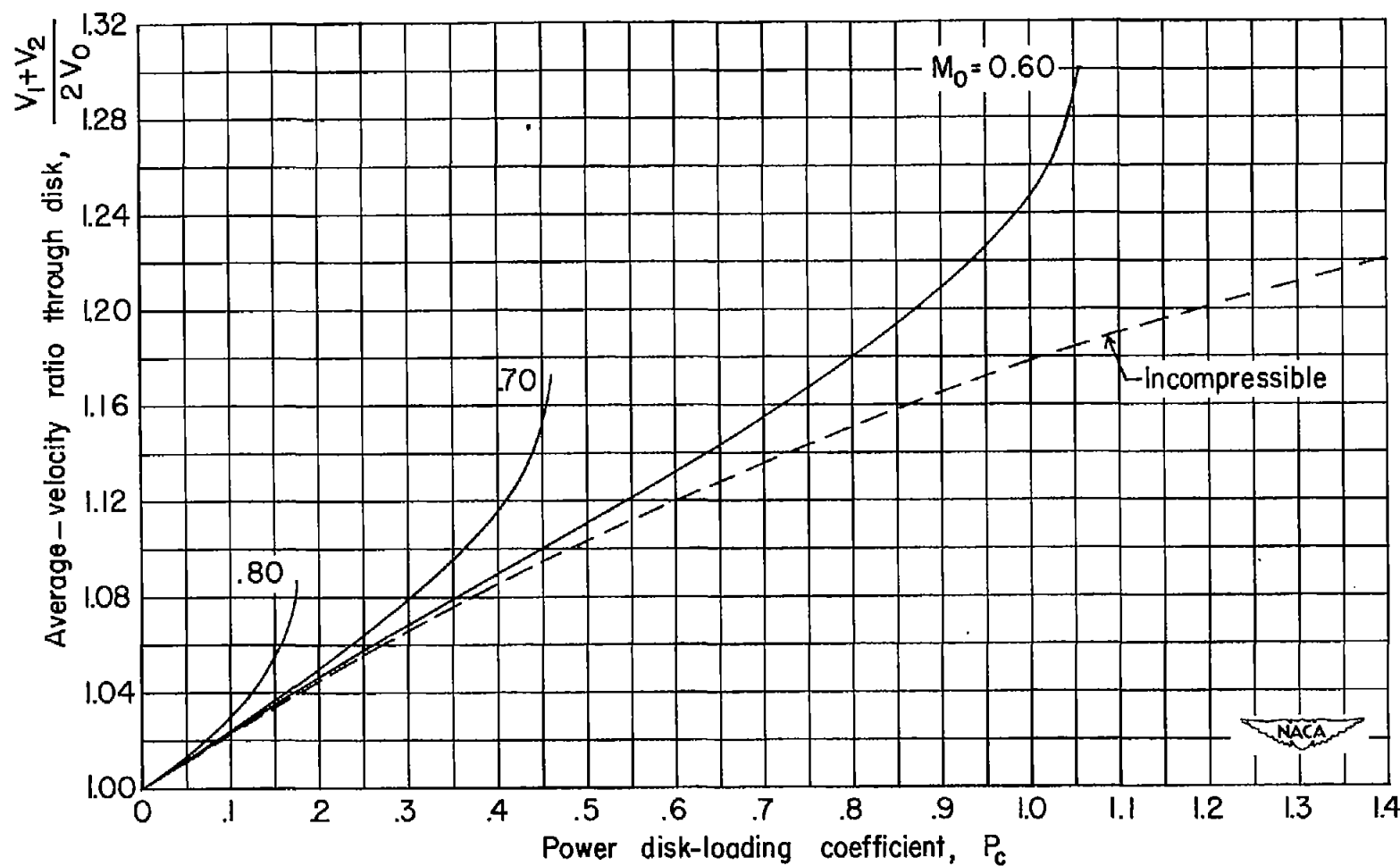
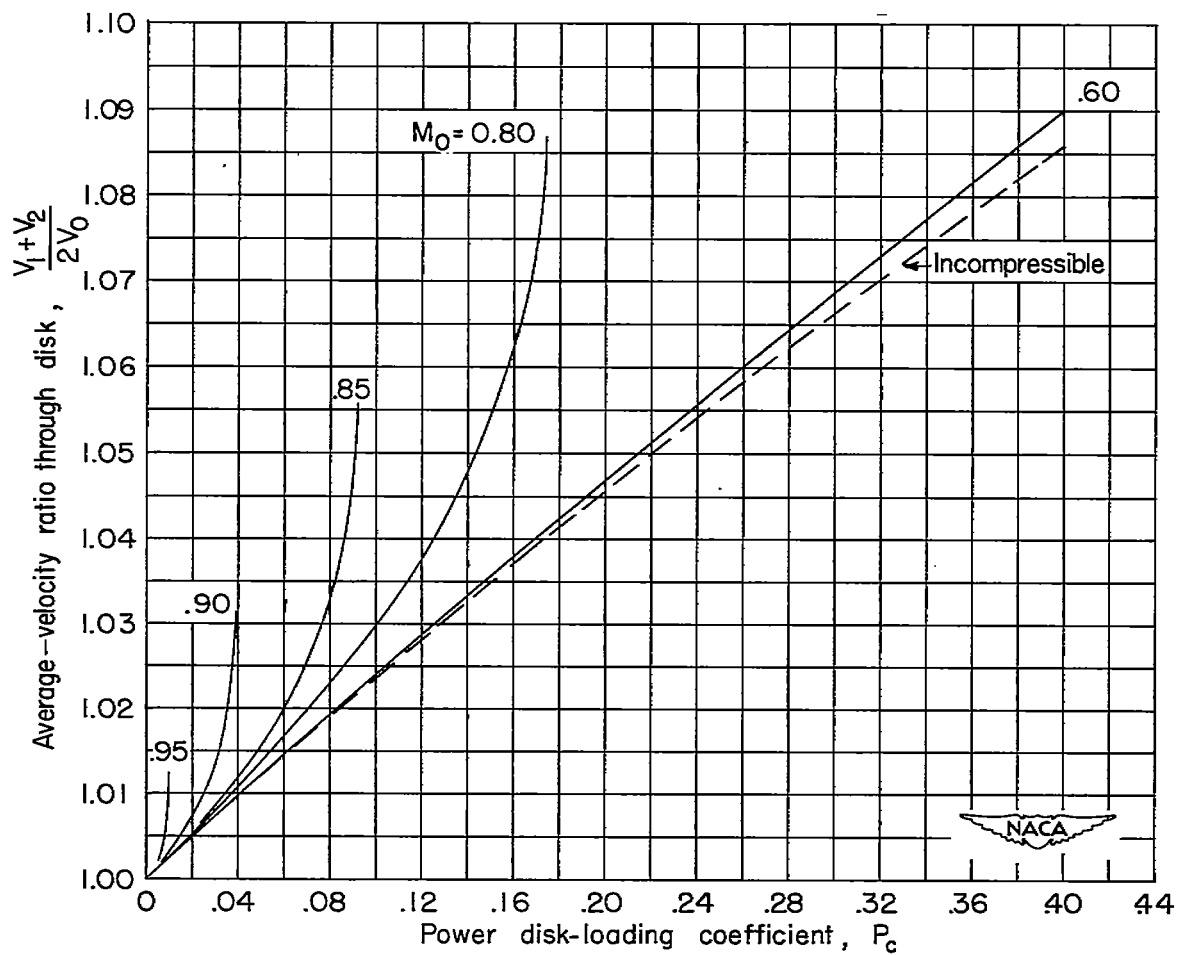


Figure 11.- Effect of free-stream Mach number on velocity ratio behind the disk. $P_0/P = 0$.



(a) $M_0 = 0.60, 0.70, \text{ and } 0.80$.

Figure 12.- Comparison of average-velocity ratio through disk for incompressible and compressible flows up to choked condition.



(b) $M_0 = 0.80, 0.85, 0.90, \text{ and } 0.95.$

Figure 12.- Concluded.

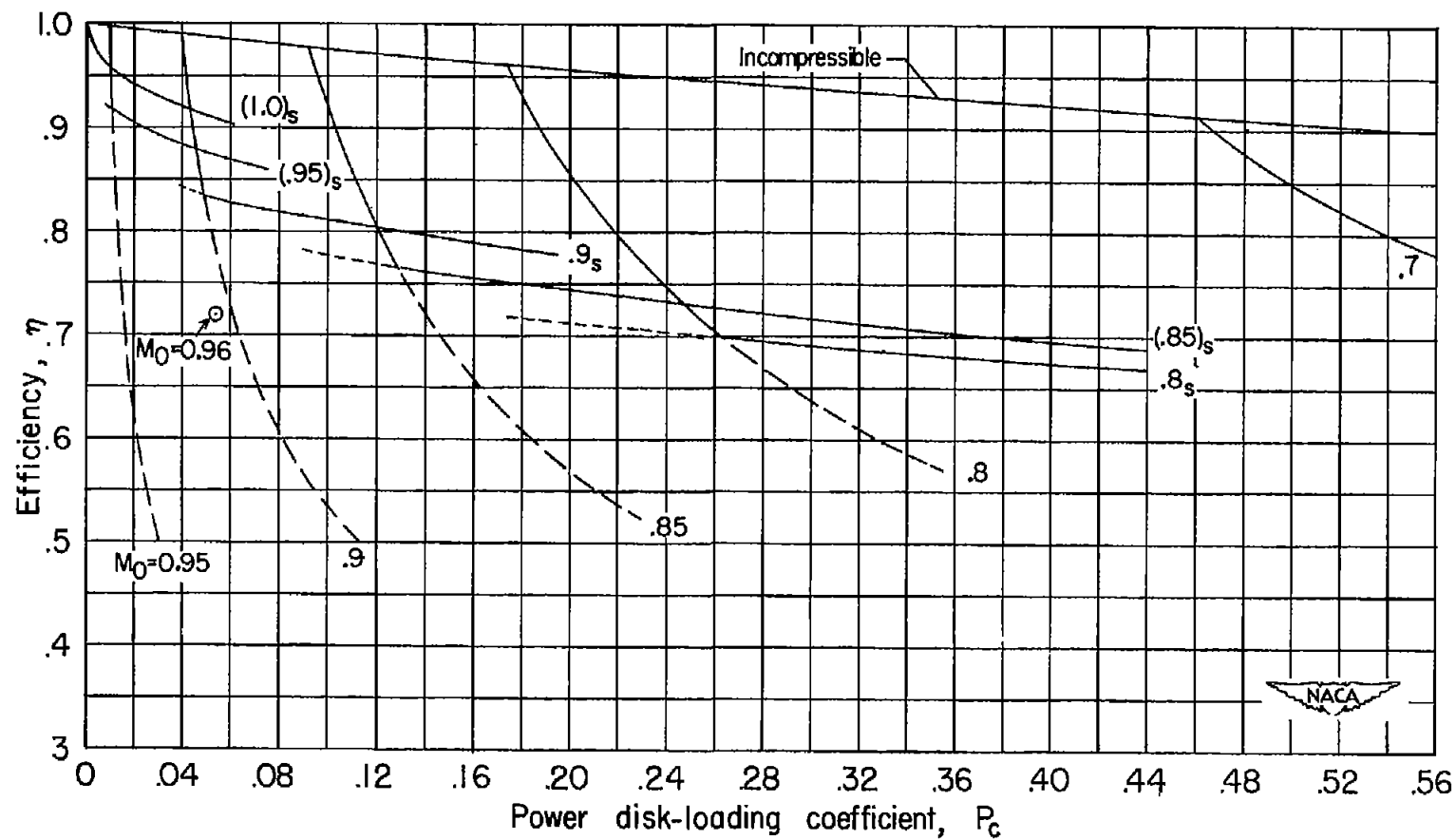
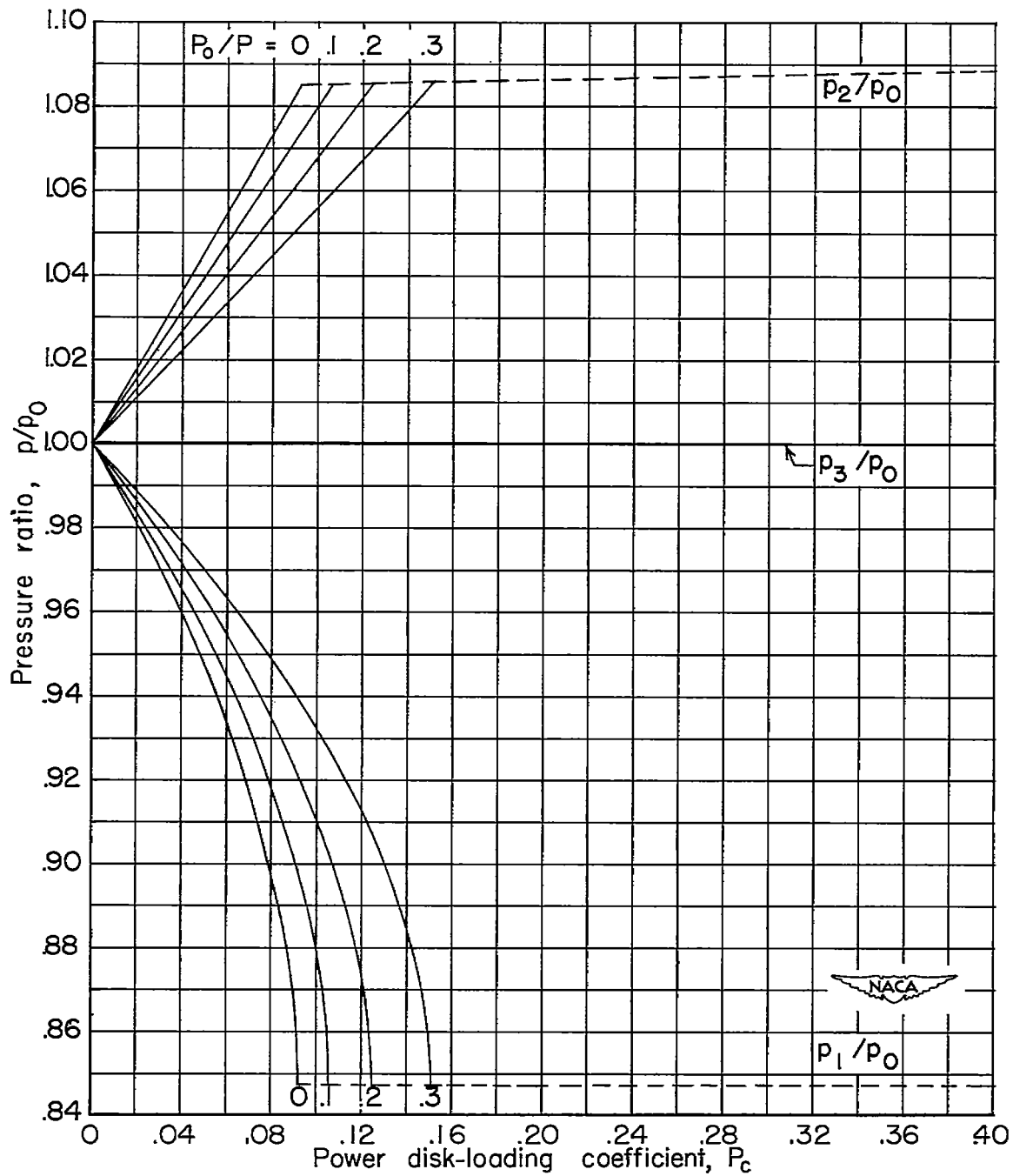
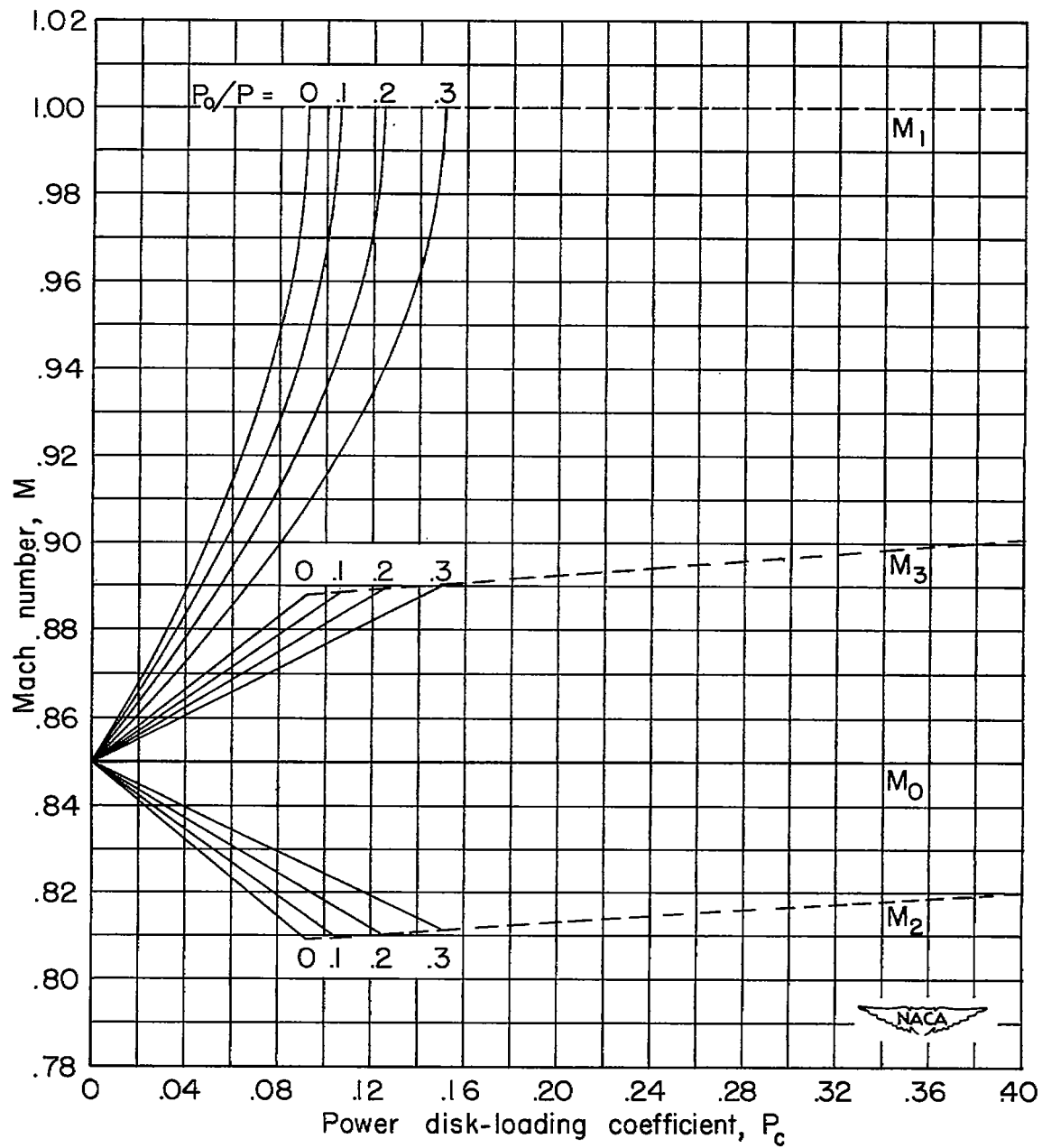


Figure 13.- Variation of maximum efficiency with power loading for several forward Mach numbers.



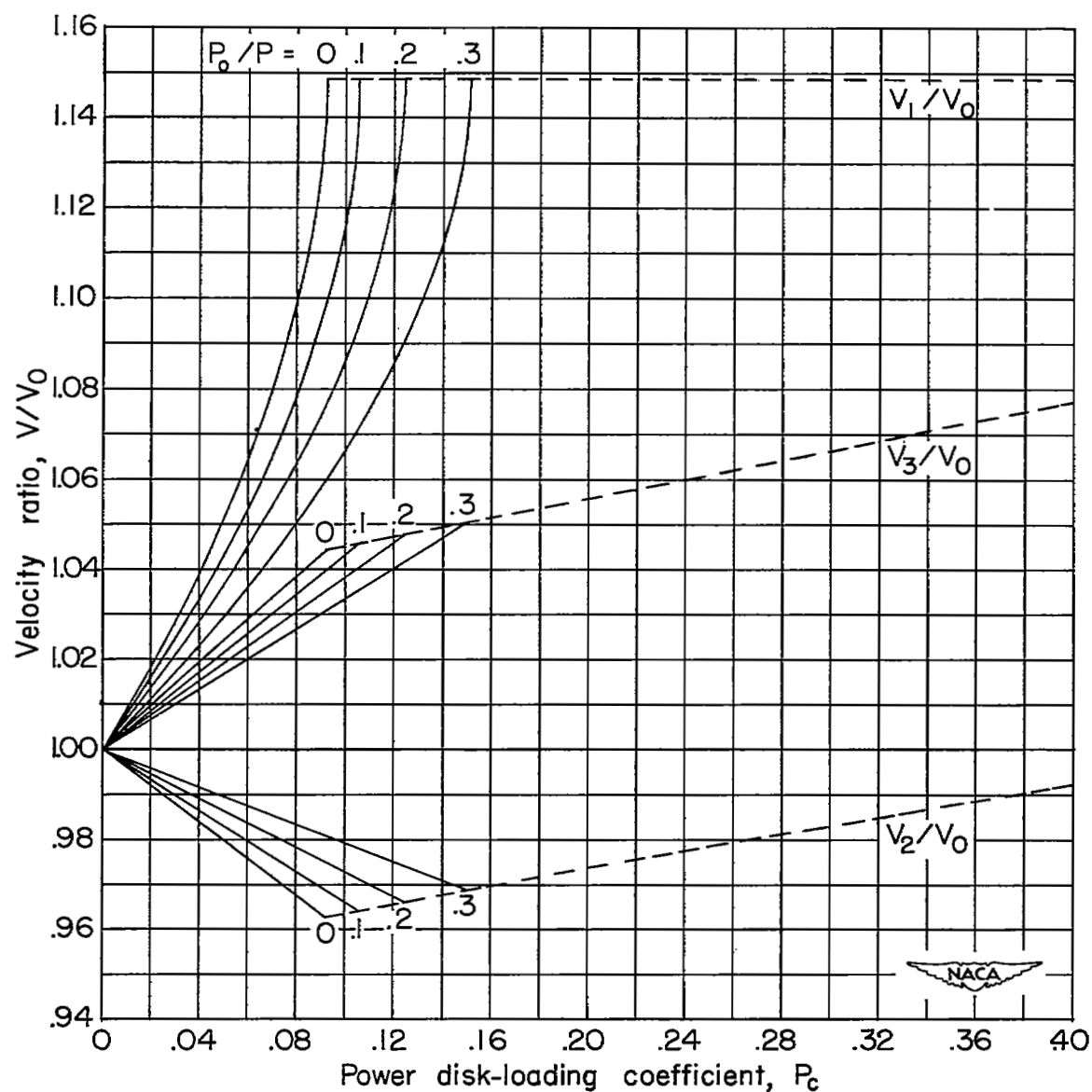
(a) Pressure ratio.

Figure 14.- Effect of profile losses on the slipstream flow factors for subsonic wake. $M_0 = 0.85$.



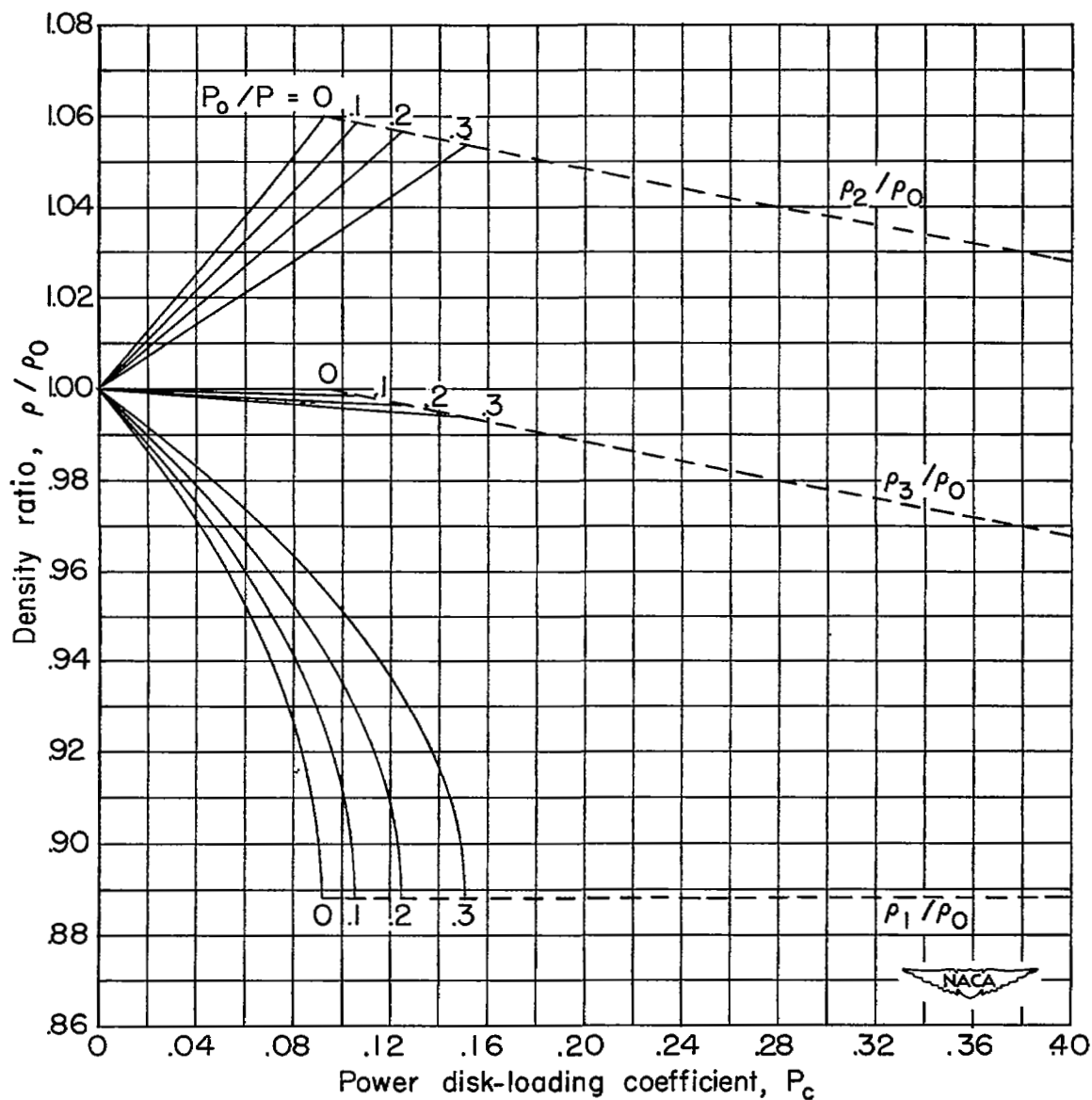
(b) Mach number.

Figure 14.- Continued.



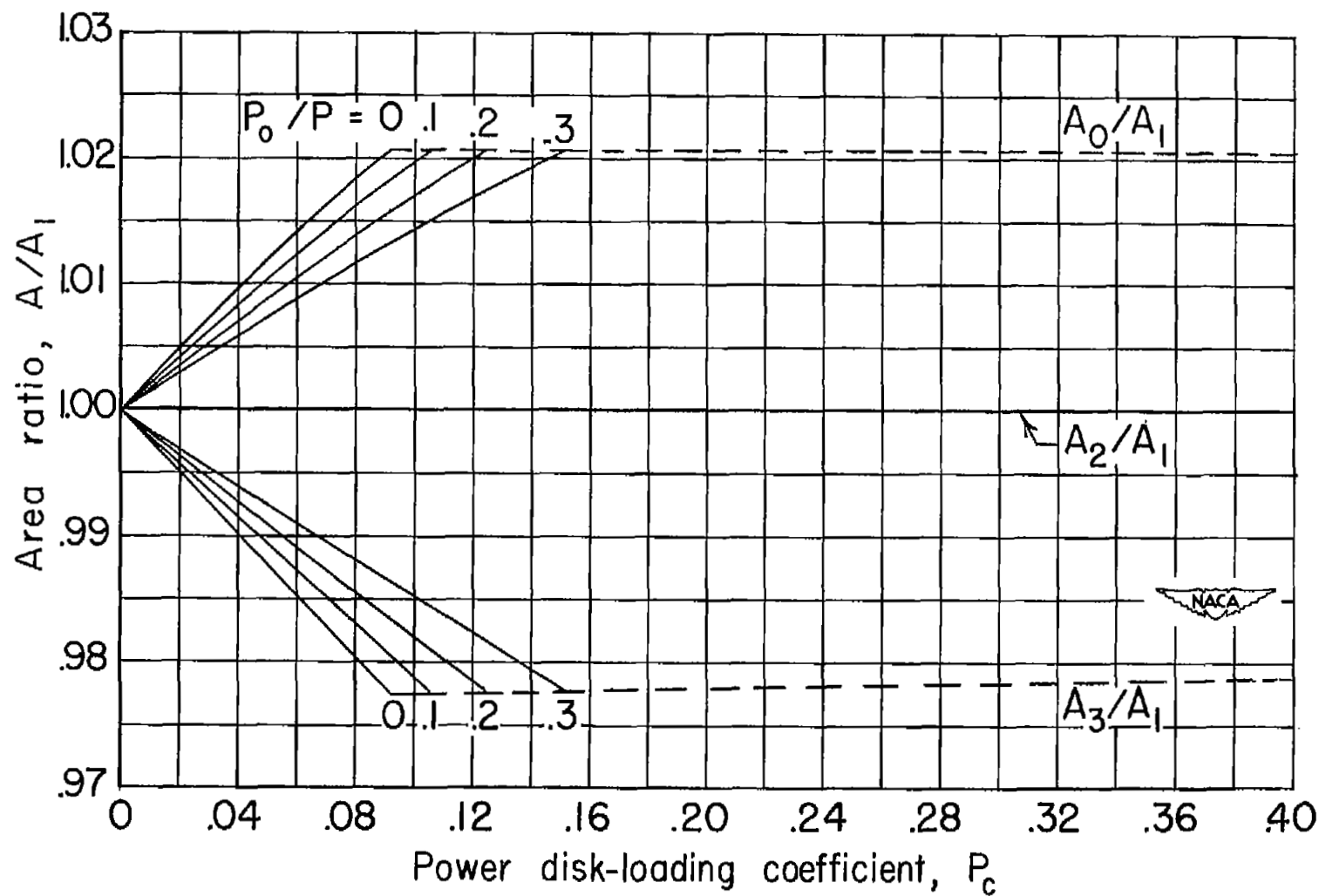
(c) Velocity ratio.

Figure 14.- Continued.



(d) Density ratio.

Figure 14.- Continued.



(e) Area ratio.

Figure 14.- Concluded.

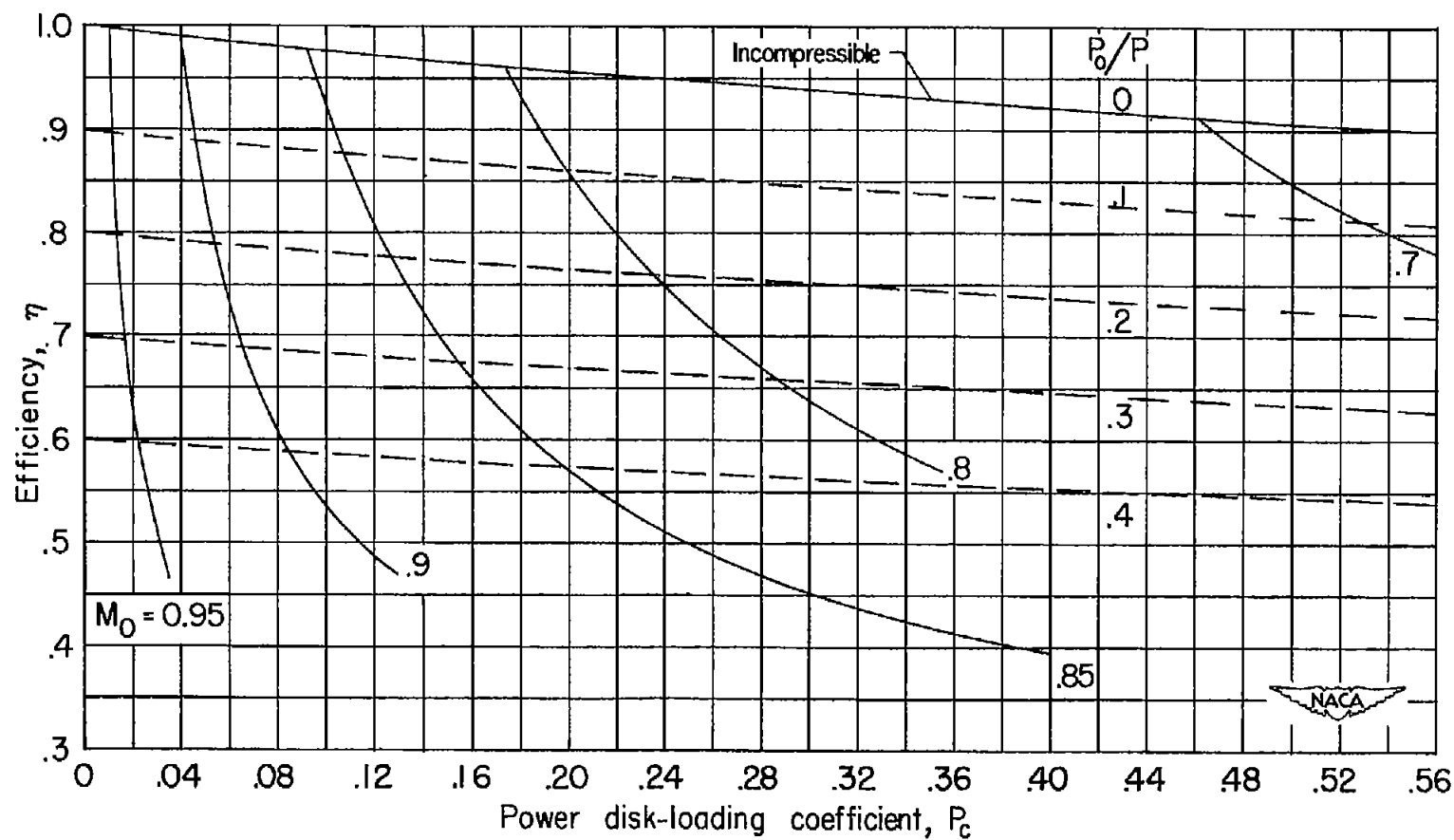


Figure 15.- Effect of profile losses on efficiency. Subsonic wake.

UNCLASSIFIED

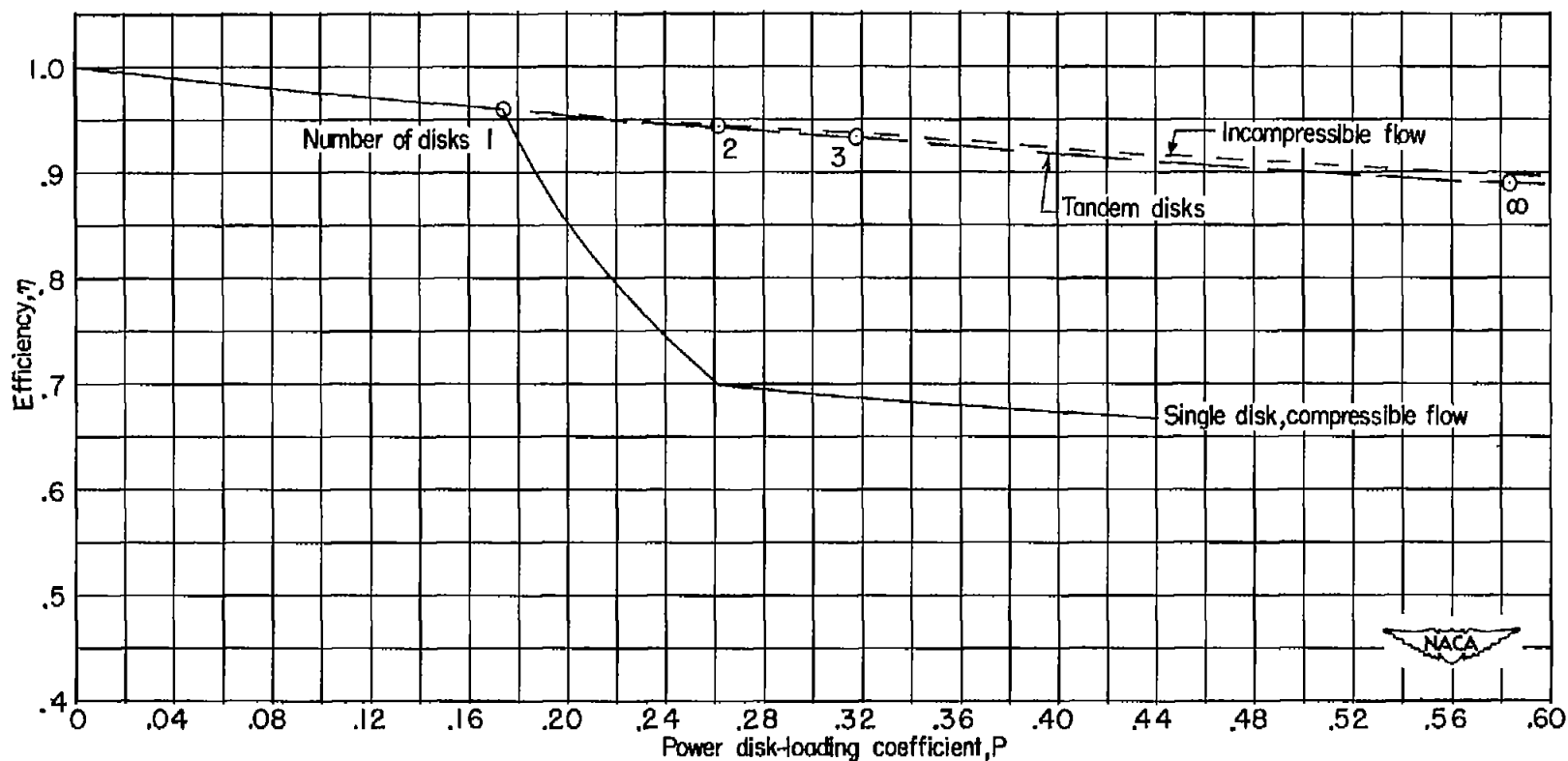


Figure 16.- Comparison of maximum efficiency for a single disk with that for an arbitrary arrangement of disks in tandem at a free-stream Mach number of 0.80.

UNCLASSIFIED

NACA RM L53A07

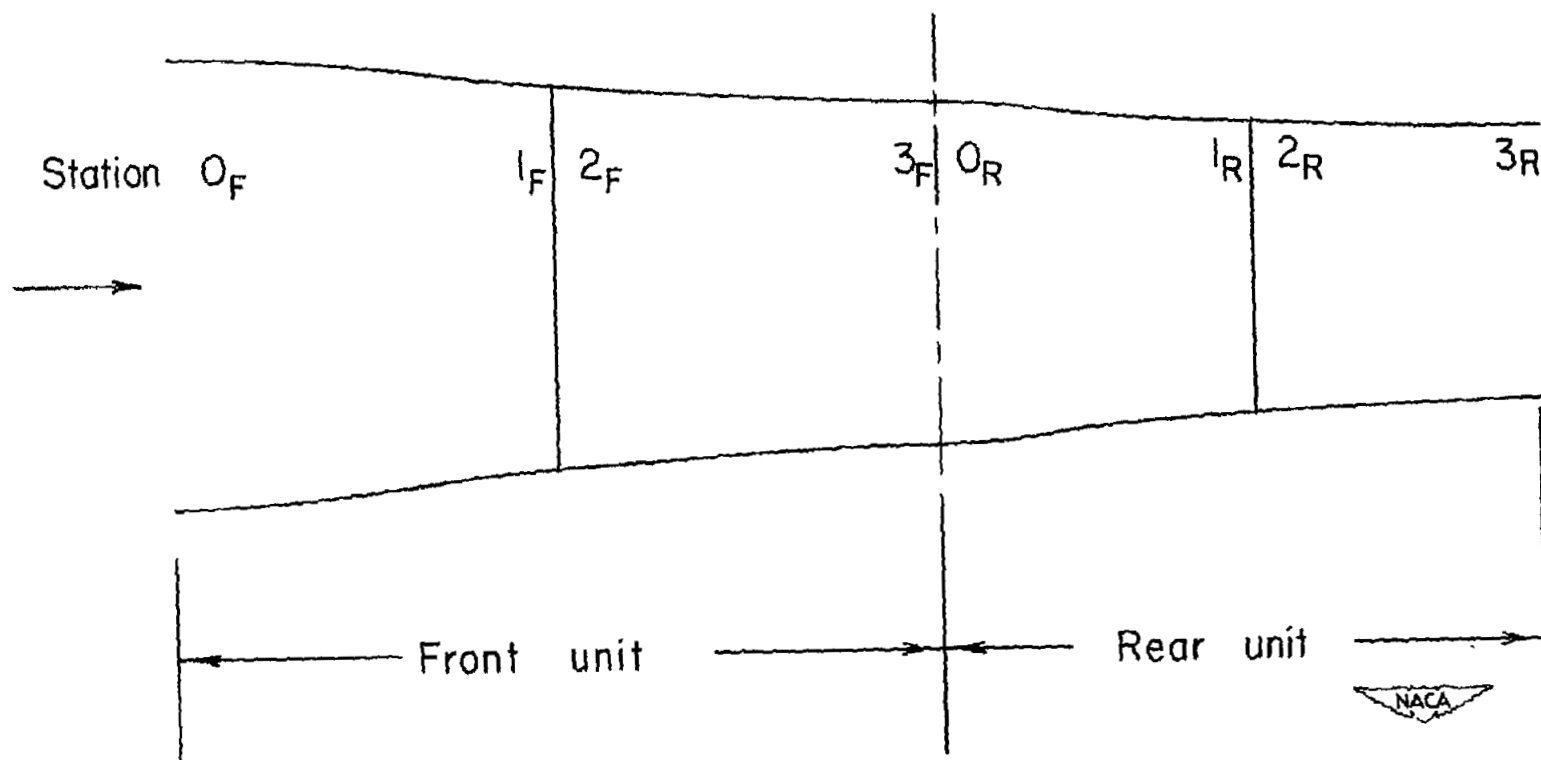


Figure 17.- Slipstream stations used in analysis of tandem actuator disks.
 (Two disks shown.) Free-stream conditions M , V , p , ρ , H , and E
 are given at station 0_F .

UNCLASSIFIED

NACA Langley - 3-20-53 - 400

SECURITY INFORMATION

NASA Technical Library



3 1176 01437 5803

UNCLASSIFIED

RESTRICTED
UNCLASSIFIED